



# Environmental factors controlling the seasonal variability in particle size distribution of modern Saharan dust deposited off Cape Blanc <sup>☆</sup>



Carmen A. Friese <sup>a,\*</sup>, Michèlle van der Does <sup>b</sup>, Ute Merkel <sup>a</sup>, Morten H. Iversen <sup>a</sup>, Gerhard Fischer <sup>a</sup>, Jan-Berend W. Stuut <sup>a,b</sup>

<sup>a</sup> MARUM – Center of Marine Environmental Sciences, Bremen University, Leobener Str., D-28359 Bremen, Germany

<sup>b</sup> NIOZ – Royal Netherlands Institute for Sea Research, Department of Ocean Systems, and Utrecht University, PO Box 59, 1790 AB Den Burg, Texel, Netherlands

## ARTICLE INFO

### Article history:

Received 31 December 2015

Revised 20 April 2016

Accepted 21 April 2016

### Keywords:

Saharan dust

Particle size spectrum

Sediment trap mooring

Wet deposition

Gravitational settling

Dust-storm

## ABSTRACT

The particle sizes of Saharan dust in marine sediment core records have been used frequently as a proxy for trade-wind speed. However, there are still large uncertainties with respect to the seasonality of the particle sizes of deposited Saharan dust off northwestern Africa and the factors influencing this seasonality. We investigated a three-year time-series of grain-size data from two sediment-trap moorings off Cape Blanc, Mauritania and compared them to observed wind-speed and precipitation as well as satellite images. Our results indicate a clear seasonality in the grain-size distributions: during summer the modal grain sizes were generally larger and the sorting was generally less pronounced compared to the winter season.

Gravitational settling was the major deposition process during winter. We conclude that the following two mechanisms control the modal grain size of the collected dust during summer: (1) wet deposition causes increased deposition fluxes resulting in coarser modal grain sizes and (2) the development of cold fronts favors the emission and transport of coarse particles off Cape Blanc. Individual dust-storm events throughout the year could be recognized in the traps as anomalously coarse-grained samples. During winter and spring, intense cyclonic dust-storm events in the dust-source region explained the enhanced emission and transport of a larger component of coarse particles off Cape Blanc. The outcome of our study provides important implications for climate modellers and paleo-climatologists.

© 2016 The Authors. Published by Elsevier B.V. This is an open access article under the CC BY license (<http://creativecommons.org/licenses/by/4.0/>).

## 1. Introduction

Mineral dust is an important component in the climate system since large amounts (~500 to ~4000 Mt) are emitted globally per year (Huneeus et al., 2011), feeding back on climate through e.g., the oceanic biological carbon pump, the atmospheric energy balance, precipitation and sea surface temperature (Maher et al., 2010; Prospero and Lamb, 2003; Stuut et al., 2008). When depos-

ited into the ocean, mineral dust can affect the efficiency of the oceanic biological carbon pump as follows: on the one hand the input of dust-related micronutrients increases the oceanic primary production leading to increased carbon fluxes (Jickells et al., 2005; Martin, 1990; Martin et al., 1991). On the other hand, the ballasting of marine snow aggregates and fecal pellets with dust minerals leads to increased densities and sinking velocities. As a consequence, the time for remineralization of organic matter in the water column is reduced resulting in an increase in the organic carbon fluxes to the deep sea (Iversen et al., 2010; Iversen and Robert, 2015; Ploug et al., 2008a).

In addition, dust emission, transport, and deposition react sensitively to climate parameters such as rainfall, wind, temperature and vegetation cover (Knippertz and Stuut, 2014). The physical and chemical characteristics of mineral dust in sediment core records can be used as a qualitative proxy for paleo-environmental conditions (Rea, 1994). However, quantitative proxy data are required in order to explain modern temporal variability in dust mobilization, transport and deposition (IPCC,

*Abbreviations:* AEJ, African easterly jet; AEWs, African easterly waves; CB, Mesotrophic sediment trap mooring; CBI, Eutrophic sediment trap mooring; CC, Canary Current; ITCZ, Intertropical Convergence Zone; MLM, Micro Liquid Module; NE, northeastern; NW, northwestern; SACW, South Atlantic Central Water; SAL, Saharan Air Layer; TEJ, tropical easterly jet.

<sup>☆</sup> <https://doi.pangaea.de/10.1594/PANGAEA.860539>.

\* Corresponding author.

*E-mail addresses:* [cfriese@marum.de](mailto:cfriese@marum.de) (C.A. Friese), [Michelle.van.der.Does@nioz.nl](mailto:Michelle.van.der.Does@nioz.nl) (M. van der Does), [umerkel@marum.de](mailto:umerkel@marum.de) (U. Merkel), [miversen@marum.de](mailto:miversen@marum.de) (M.H. Iversen), [gfisher@marum.de](mailto:gfisher@marum.de) (G. Fischer), [jbstuut@marum.de](mailto:jbstuut@marum.de), [Jan-Berend.Stuut@nioz.nl](mailto:Jan-Berend.Stuut@nioz.nl) (J.-B.W. Stuut).

<http://dx.doi.org/10.1016/j.aeolia.2016.04.005>

1875-9637/© 2016 The Authors. Published by Elsevier B.V.

This is an open access article under the CC BY license (<http://creativecommons.org/licenses/by/4.0/>).

## Nomenclature

### Mathematical abbreviations

$D$	Particle diameter
$g$	Acceleration due to gravity
$KD^2$	Settling velocity
$L$	Distance traveled by a suspended particle

$U$	Wind speed
$\varepsilon$	Coefficient of turbulent exchange
$\rho_s$	Density of the particle
$\mu$	Dynamic viscosity of air

2007; Stuu et al., 2008). This information is needed to facilitate the paleoclimatic interpretation of dust in sedimentological records (Caquineau et al., 2002; Scheuven et al., 2013; Stuu et al., 2005) and to test the representation of the dust cycle in climate models, which are also applied for future climate scenario simulations (Huneus et al., 2011; Luo et al., 2003; Mahowald et al., 2003).

In the dust-source region, a certain threshold wind velocity is required to mobilize dust particles. The uplift of coarse dust particles and aggregates larger than  $20\ \mu\text{m}$  up to heights of 100 m only occurs during intense dust storms and so-called ‘haboobs’ (Tsoar and Pye, 1987). Prospero et al. (1970) related an anomalously coarse spring dust sample obtained at Barbados to a single African dust storm using satellite photographs. Furthermore, Rea (1994) hypothesized that giant quartz grains in sediment-core records reflect individual high-energetic dust storms. More grain-size data are required to test the hypothesis whether dust storm events as depicted on satellite images are reflected in depositions of anomalously coarse dust downwind from the dust source.

Transport processes can alter the initial particle-size distribution of the released mineral dust. The mean diameter of suspended dust decreases exponentially with atmospheric height (Tsoar and Pye, 1987). The mean grain size of dust particles decreases horizontally with increasing transport distance due to the preferential gravitational settling of coarser particles (Darwin, 1846; Holz et al., 2004). Furthermore, the transport distance of dust particles increases linearly with wind speed (Tsoar and Pye, 1987). Coarser

grain sizes of deposited dust in sediment-trap records offshore Cape Verde and in onland dust collectors at M’bour (Senegal) during boreal summer have been related to the seasonal change in the altitude of the dust transport (Ratmeyer et al., 1999a; Skonieczny et al., 2013). According to these studies, higher-altitude transport of Saharan dust ( $\sim 3\ \text{km}$  height) during summer led to the deposition of a larger percentage of coarser particles at the sampling sites, while most finer particles remained in suspension and could be transported across the Atlantic to the Caribbean (Carlson and Prospero, 1972). Again, more grain-size data are required to test this hypothesis.

Whereas dry deposition includes the preferential gravitational settling of coarse particles, wet deposition after in-cloud scavenging results in the settling of increased amounts of submicron particles (Jung and Shao, 2006). Dust deposited during summer-rain events at the sampling site M’bour (Senegal) (Fig. 1) features a larger volume percentage of fine particles  $<10\ \mu\text{m}$  (Skonieczny et al., 2013). These latter authors relate the larger component of finer particles to the scavenging of these smaller particles from higher altitudes due to precipitation.

We hypothesize that a complex interplay of factors including transport and depositional processes and the wind speed in the source region are responsible for seasonal variations in the modal grain size of deposited Saharan dust. We therefore investigated a dataset of dust deposited in sediment-traps off Cape Blanc between 2003 and 2006. Based on grain-size analysis and meteorological data as well as satellite images, we aim to answer the following questions:

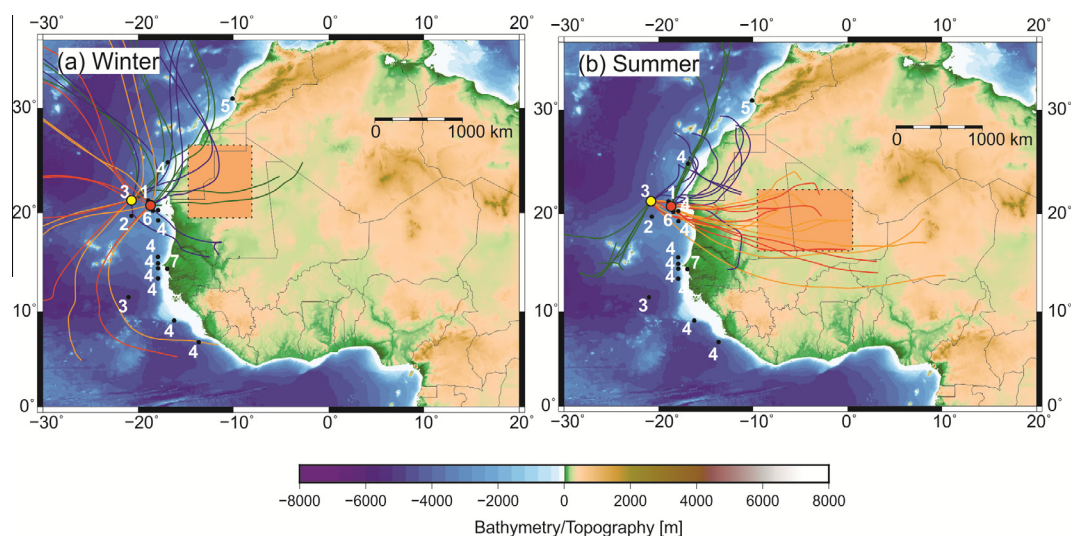


**Fig. 1.** Locations of the sediment-trap moorings CB (yellow circle) and CBi (red circle) offshore Cape Blanc and the environmental conditions during boreal winter (a) and boreal summer (b) in the area under investigation. Note the seasonal change in predominant dust source regions (orange boxes, illustrated after Stuu et al. (2005), Goudie and Middleton (2001), Knippertz and Todd (2010), Schepanski et al. (2007)) and 3-day back-trajectories (red lines = 5500 m altitude, orange lines = 3000 m, dark blue lines = 1000 m, darkgreen lines = 10 m ending on 01.02.2006 (a) and 30.08.2003 (b), calculated using the HYSPLIT Trajectory model on the NOAA website at: <http://ready.arl.noaa.gov>). The study sites of other authors are also indicated (black circles, 1 = Koopmann, 1981; 2 = Matthewson et al., 1995; 3 = Ratmeyer et al., 1999a,b; 4 = Stuu et al., 2005; 5 = McGregor et al., 2009; 6 = Filipsson et al., 2011; 7 = Skonieczny et al., 2013). (For interpretation of the references to color in this figure legend, the reader is referred to the web version of this article.)

- (1) What is the seasonal variability in particle size of mineral dust in marine sediments over the period 2003–2006?
- (2) Can we distinguish dust-storm events, observed from satellite images, from background dust in marine sediments based on (modal) particle size?
- (3) What is the influence of meteorological parameters (wind speed, precipitation) on the modal particle size of dust in marine sediments off Cape Blanc?

## 2. Study site

### 2.1. Atmospheric setting

The sediment trap mooring sites CB (mesotrophic,  $\sim 21^{\circ}16' N$ ,  $\sim 20^{\circ}48' W$ ) and CBI (eutrophic,  $\sim 20^{\circ}45' N$ ,  $\sim 18^{\circ}42' W$ ) are positioned in the northeastern (NE) equatorial Atlantic Ocean offshore Cape Blanc (Mauritania) at about 200 and 80 nautical miles from the coast, respectively. This region offers an excellent opportunity to study modern dust mobilization, transport, and deposition since about 50 Mt of dust are deposited between the African coast and  $35^{\circ}W$  each year (Yu et al., 2015). An additional advantage of this study area is the lack of fluvial input (Ratmeyer et al., 1999b).

The meteorology of the study area is controlled by the seasonal variability in insolation. Over the western African continent the core of the Intertropical Convergence Zone (ITCZ) shifts meridionally from  $\sim 12^{\circ}N$  during winter to  $\sim 21^{\circ}N$  during summer (Nicholson, 2009). This implies a seasonal change in precipitation and winds over the African continent, which is strongly related to dust mobilization and transport offshore Cape Blanc (Prospero and Nees, 1977). Rainfall at about  $20^{\circ}N$  (latitude of our study site) is most intense during summer and fall in West Africa and is related to the monsoon and the northward propagating ITCZ. During late summer the rain belt is associated with a large core of rising air lying between the African easterly jet (AEJ) and the tropical easterly jet (TEJ), a region which corresponds to the southern track of the African easterly waves (AEWs) at  $\sim 10^{\circ}N$  (Nicholson, 2009). A smaller branch of rising air with smaller amounts of rainfall exists in the region of the surface expression of the ITCZ and the northern track of the AEWs at  $\sim 21^{\circ}N$  (Nicholson, 2009).

During boreal winter, dust is transported predominantly from Mauritania and the coastal areas of Western Sahara to the sediment-trap mooring sites within the low-level NE trade winds, which are part of the large-scale northern Hadley cell (Hamilton and Archbold, 1945; Stuut et al., 2005) (Fig. 1a). The maximum wind speed of the NE trade winds is  $\sim 50 \text{ km h}^{-1}$  near the surface,

however NE winds blow up to altitudes of 3 km (Fig. 2a) (Stuut et al., 2005). Dry NE surface winds laden with dust on the African continent are locally known as ‘Harmattan’, which translates to ‘wind that carries dust’ (Dobson, 1781). Strong dust-storm events during winter may evolve due to the penetration of cold air with high wind velocities from higher latitudes to lower latitudes (Knippertz and Fink, 2006).

During boreal summer, the main source area for dust transported offshore northwestern (NW) Africa is the Sahel, especially Mauritania and Mali (Knippertz and Todd, 2010; Middleton and Goudie, 2001; Schepanski et al., 2007) (Fig. 1b). The lower atmosphere is characterized by NE trade winds, which transport significant amounts of dust when having an overland trajectory (Carlson and Prospero, 1972). In the Caribbean, Saharan air has been identified as an isentropic layer of warm and dry air bordered by two strong inversions. This layer of Saharan air has been denoted the ‘Saharan Air Layer’ (SAL) based on its continental origin, characteristics, and spatial homogeneity (Carlson and Prospero, 1972; Diaz et al., 1976; Prospero and Carlson, 1972). The SAL frequently contains high dust concentrations and is situated between  $\sim 0.6 \text{ km}$  (950 hPa) and  $\sim 5.5 \text{ km}$  (500 hPa) offshore NW Africa (Carlson and Prospero, 1972; Prospero and Carlson, 1970). Strong dry boundary layer convection on the African continent during summer and fall leads to the entrainment of dust into the SAL. When the ITCZ and the low-level monsoonal flow move northwards, the dust-containing SAL is lifted above the cooler monsoonal air masses. The AEJ blowing at an altitude of  $>3 \text{ km}$  (700 hPa) leads to a westward movement of the SAL and accompanying dust particles (Carlson and Prospero, 1972). The strength and direction of the dust transport is also connected to the passage of AEW disturbances (Jones et al., 2003). On satellite images (Fig 2b), the Saharan air including the dust front can be observed in a relatively cloud-free area away from the AEW track which exhibits pronounced bands of clouds. Wind velocities within the SAL are maximum at an altitude of  $\sim 3\text{--}4 \text{ km}$  (600–700 hPa) with  $70 \text{ km h}^{-1}$  in the area of the Cape Verde islands (Carlson and Prospero, 1972). Amplified moist convection during summer can trigger strong dust-storm events, or haboobs (Knippertz and Todd, 2010).

During spring, dust-storm events occur most frequently and dust is sourced from a large area centered on Mauritania and Mali (Middleton and Goudie, 2001). This is also the season of generally high dust deposition fluxes on the Senegalese margin (Skonieczny et al., 2013). During spring, cyclonic storms favoring the emission of dust occur more frequently over the African continent owing to the large temperature contrast between the cold mid- and high

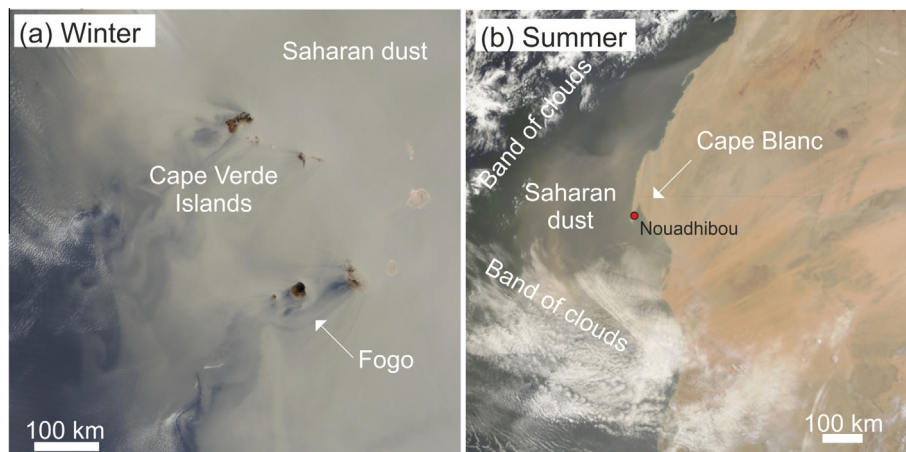


**Fig. 2.** (a) Satellite image showing a winter low-level dust outbreak captured on 5 March 2004. The volcano of the Cape Verde Island Fogo (altitude 2829 m) sticks through the dust plume. (b) Satellite image showing a summer dust outbreak on 23 July 2006. Saharan dust is situated to the east of a dense band of clouds. Both images © NASA Earth Observatory.

**Table 1**  
Specifications of the six sediment trap series CB and CBI.

Sediment trap series	Trap type	Sampling period	Cruise deployment	Cruise recovery	Position	Trap depth [m]	Water depth [m]	No. of samples	Sampling intervals
CBi 1 upper	SMT 243	05.06.2003–05.04.2004	M58/2	Pos310	20°45.0' N 18°42.0' W	1296	2714	20	1 × 10.5d + 19 × 15.5d
CBi 2 upper	SMT 230	18.04.2004–20.07.2005	Pos310	M65/2	20°44.7' N 18°42.1' W	1296	2714	16	1 × 22d + 14 × 23d + 1 × 22d
CBi 3 upper	SMT 230	25.07.2005–25.07.2006	M65/2	Pos344	20°45.6' N 18°41.9' W	1277	2693	17	17 × 21.5d
CB 14 upper	SMT 243	31.05.2003–02.11.2003 (Cups 11–20 could not be used)	M58/2	Pos310	21°17.2' N 20°47.6' W	1246	4162	10	10 × 15.5d
CB 15 lower	SMT 234	18.04.2004–20.07.2005	Pos310	M65/2	21°17.9' N 20°47.8' W	3624	4162	20	20 × 23d
CB 16 lower	SMT 230	25.07.2005–28.09.2006	M65/2	Pos344	21°16.8' N 20°47.8' W	3633	4160	20	20 × 21.5d

latitudes and quickly heating subtropical landmasses (Knippertz, 2014). During fall, atmospheric dust loadings are generally low (Knippertz and Todd, 2012).

## 2.2. Oceanic setting

The surface water circulation offshore Cape Blanc is influenced by two wind-driven surface currents: The southward-flowing Canary Current (CC) and the poleward-flowing coastal countercurrent or Mauritania current. Owing to the seasonal shift in atmospheric circulation the surface currents shift seasonally off Cape Blanc. During winter and spring, the sediment-trap mooring locations are overlain by the CC which becomes detached from the continental margin at these latitudes. During summer, the mooring locations are within the influence of the poleward flowing coastal countercurrent. Below, the deeper water masses include the poleward flowing undercurrent extending down to water depths of 1000 m (Mittelstaedt, 1991). The poleward flowing South Atlantic Central Water (SACW) is situated below the countercurrent (Mittelstaedt, 1991).

As has been shown by previous studies, the grain sizes of aerosol samples, sediment trap and surface sediments at site CB resemble each other well, hence horizontal advection of particles in the water column while sinking towards the sea floor is considered minimal (Ratmeyer et al., 1999b; Stuu et al., 2005). In addition, deep-sea sediment-trap studies in combination with particle-camera investigations at site CBI suggest that little particle transformations occur between the surface waters and the deep ocean (Nowald et al., 2015). At site CB, particles have been estimated to sink with a high mean settling speed of  $\sim 240 \text{ m d}^{-1}$  (Fischer and Karakas, 2009). High particle sinking velocities in the study area are the result of aggregate formation and ballasting of the marine snow aggregates and fecal pellets with dense carbonate, opal and Saharan dust particles (Fischer and Karakas, 2009; Iversen et al., 2010; Iversen and Ploug, 2010; Iversen and Robert, 2015; Ploug et al., 2008b). Aggregate formation and ballasting is most important in the surface waters (less than 250 m water depth) (Iversen et al., 2010). The incorporation of dust particles in larger marine aggregates and fecal pellets is the mechanism by which fine-grained dust particles are transported from the surface ocean to the deep sea (Ternon et al., 2010).

## 3. Material and methods

### 3.1. Sediment-trap samples

The samples of six sediment-trap deployments at the sediment trap mooring stations CB (mesotrophic) and CBI (eutrophic) during 2003–2006 were chosen for grain-size analyses (Table 1). The

distance between the sampling locations CB and CBI is  $\sim 250 \text{ km}$ . The upper traps of site CB and CBI sampled at a water depth of  $\sim 1300 \text{ mbsl}$ . The lower trap at site CB sampled at a water depth of  $\sim 3600 \text{ mbsl}$ .

The sediment traps are conical and of the type Kiel (model SMT-230/234/243) with an opening of  $0.5 \text{ m}^2$  and fitted with a  $1 \text{ cm}^2$  grid at the top. Twenty sample cups rotated according to a pre-programmed sampling interval (Fischer and Wefer, 1991). The sampling intervals of the traps were synchronized between the two mooring stations during most of the time, enabling an excellent comparison between the two sites. The sampling interval ranged from 10.5 days to 23 days (Table 1). Deployment and recovery of the chosen sediment-trap samples was executed during the expeditions M58/2, POS310, M65/2 and POS344 (Bleil et al., 2006; Fischer and Ruhland, 2008; Krastel, 2006; Meinecke, 2005). Individual working steps related to trap deployment and treatment are described in Fischer and Wefer (1991). Prior to deployment, the sampling cups were filled with ambient seawater. 100 g NaCl suprapur was added to 1 l seawater and from this 20 ml was added to each sample cup to increase the salinity from 35‰ to 40‰. As a result, the water density inside the cups was larger than the ambient seawater leading to minimized outflow of water during sampling. Further, the cups were poisoned with 1 ml of a saturated solution of  $\text{HgCl}_2$  in seawater per 100 ml of filtered seawater. Consequently, microbial and zooplankton activity in the samples was inhibited, which can alter the sediments via organic material consumption and particle remineralization (Buesseler et al., 2007; Fischer et al., 1996). After recovery, the particulate material was sieved through a 1 mm mesh to remove swimmers. Subsequently, the samples were split into five equal aliquots with the aid of a McLane rotary liquid splitter. For grain-size analysis, 1/25 split of the original sample was used.

When interpreting sediment-trap data the following possible limitations and biases should be taken into account. First, ocean currents and the tilt of the sediment trap affect the particle collection efficiency: for current velocities  $> 12 \text{ cm s}^{-1}$  the collection efficiency decreases with increasing current speed and with decreasing particle mean diameter and settling velocity (Baker et al., 1988). However, Aanderaa current meter data from mooring site CB reveal current velocities rarely exceeding  $12 \text{ cm s}^{-1}$  at water depths of  $\sim 3600 \text{ m}$  (Helmke et al., 2005), and a study on the trapping efficiency of several sediment traps moored at different depths indicates that significant undertrapping only occurs at less than 1200 m water depth (Yu et al., 2001). Second, the exact collection area of the traps cannot be determined accurately since there are no quantitative particle settling rates and horizontal advection data available for the area. Hence, limitations in the comparison of trap data with local meteorological data should be considered. Assuming a mean particle vertical settling velocity of

240 m d<sup>-1</sup> (Fischer and Karakas, 2009) and a mean horizontal current speed of 3.75 cm s<sup>-1</sup> (Mittelstaedt, 1991), the horizontal length scale of the upper trap catchment is roughly 20 km whereas the lower trap at site CB might have a horizontal length scale of roughly 50 km. This is in agreement with the findings of Siegel et al. (1990), giving a general horizontal length scale of approximately 15–60 km for a trap at 1000 m and 60–120 km for a trap at 4000 m water depth.

### 3.2. Grain-size analysis

Grain-size analyses (see also Filipsson et al. (2011), Meyer et al. (2013) and Stuut (2001) for methodology) were carried out to analyze transport and deposition of Saharan dust. However, the recovered sediments consisted not only of mineral dust but also of a large proportion of biogenic silica, calcium carbonate, and organic material originating from marine plankton. In order to isolate the lithogenic material, which is the fraction of interest in the samples, all biogenic material was removed with the following chemical-pretreatment steps: (1) the organic matter was oxidized by adding 10 ml H<sub>2</sub>O<sub>2</sub> (35%) to the sediment sample and by subsequently boiling the sample until the reaction stops, (2) calcium carbonate was dissolved by adding 10 ml HCl (10%) to the sediment sample and by subsequently boiling the mixture for exactly 1 min and (3) biogenic silica was dissolved via adding 6 g of NaOH pellets to the sediment sample and by boiling the mixture for 10 min. Before analysis, each sample was boiled shortly with 10 drops of Na<sub>4</sub>P<sub>2</sub>O<sub>7</sub>·10H<sub>2</sub>O and stirred to assure the full disaggregation of the particles. The samples of CBI-3 were centrifuged in order to speed up the laboratory work. However, after centrifugal treatment, some samples developed aggregates. Hence, additional treatment in the ultrasonic bath for one minute was required for the samples of CBI-3 to assure disaggregation. Each sample was analyzed using the laser particle sizer Beckmann Coulter LS13320 with addition of a Micro Liquid Module (MLM) since this instrument allows quick, accurate, and precise data acquisition of large size intervals (Stuut, 2001).

Laser-diffraction particle sizers have been shown to produce accurate and precise measurements of glass-bead standards and mixtures of those [Stuut, 2001]. The precision of the instrument and systematic errors with respect to the modal grain size have been estimated using an internal glass-bead standard A6. The mean precision of the instrument is ±1.26 μm (±4.00%) for the measured modal grain size range of our samples (10–55 μm). The systematic error with respect to the detector center 31.51 μm can be as large as +3.08 μm (+9.77%), while the mean deviation is only +0.84 μm (2.67%) which is below the mean estimated instrument precision. Hence, an analytical error of ±1.26 μm (±4.00%) was considered for the results. The accuracy of the grain-size distributions has been verified by measuring the external standard G15 offered by Beckmann Coulter. The resulting mean and standard deviations of the grain-size distributions were within the limits given by the company.

### 3.3. Satellite images and meteorological data

The obtained grain-size time-series of the upper trap deployments CBI 1–3 was correlated to available local meteorological data (wind speed, precipitation) and compared with available near-by continental meteorological data (dew point, temperature, wind direction, wind speed, pressure, visibility). In addition, the grain-size time-series was compared to available satellite quasi-true color images.

Local daily zonal wind-speed data (20th Century Reanalysis V2 dataset) for specific atmospheric levels was provided by the NOAA physical science division, Boulder, Colorado, USA on their web site

(<http://www.esrl.noaa.gov/psd>). The zonal wind speed was downloaded for the atmospheric levels 1010 hPa to 500 hPa using a grid point in the dataset (22°N, 20°W) with coordinates closest to mooring station CBI (~20°45' N, ~18°42' W). Local daily precipitation data (TRMM dataset) was taken from the Giovanni online data system, developed and maintained by the NASA GES DISC (<http://gdata1.sci.gsfc.nasa.gov>). The daily precipitation data was downloaded as area-averages around CBI (20°33' – 20°48' N, 18°36' – 18°43' W) according to the assumed catchment area of the upper trap (40 × 40 km<sup>2</sup>).

Continental hourly weather data from the Nouadhibou meteorological station (20°55' N, 17°1' W) (see Fig. 2b for the location of Nouadhibou) was ordered online from the Cedar Lake Ventures website (<https://weatherspark.com>). Satellite quasi-true color RGB images (MODIS dataset) were provided by the NASA Ocean Biology Distributed Active Archive Center (OB.DAAC), Goddard Space Flight Center, Greenbelt MD on their website (<http://oceancolor.gsfc.nasa.gov>).

## 4. Results

### 4.1. Grain-size analysis

#### 4.1.1. Grain-size distributions

The Coulter LS13320 laser particle sizer was used to measure the frequency of each particle-size bin (particle diameter) in volume percentages. For the calculation of the particle volume each particle was assumed to be spherical (Syvitski, 1991). In Fig. 3 typical winter and summer grain-size frequency distributions are shown. The seasons were defined based on the astronomical calendar. Measured particle sizes ranged from 0.4 μm to 250 μm. Particles smaller than 0.4 μm could not be detected by the Coulter laser particle sizer. A common characteristic of the measured grain-size distributions was the coarse shoulder in the size spectrum between ~100 and 250 μm. This has been observed before (Glaccum and Prospero, 1980) and is related to the platy shape of mica particles with an aerodynamic size smaller than their optical size (Stuut et al., 2005). The particle-size distribution of the summer samples was generally wider and showed larger volume percentages of submicron particles and particles with sizes above 100 μm compared to the winter distributions. Hence, the standard deviation (σ) was larger for the summer samples than for the

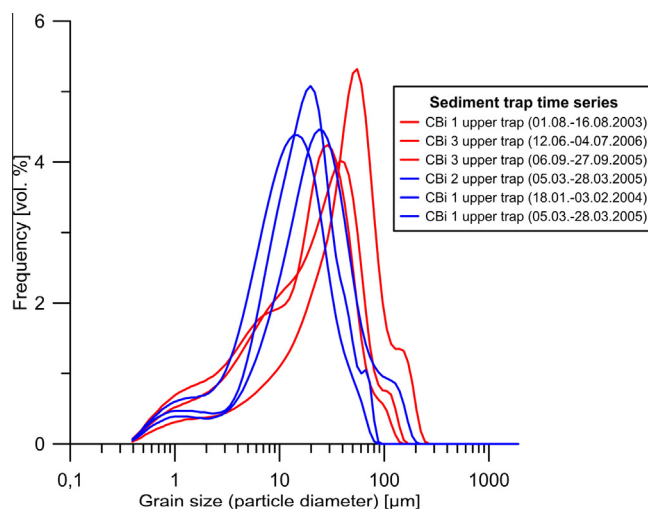


Fig. 3. Selected examples for typical summer (red) and winter (blue) grain-size distributions from the upper trap series (1–3) at the eutrophic sediment trap site CBI. (For interpretation of the references to color in this figure legend, the reader is referred to the web version of this article.)

winter samples. The standard deviation is a measure of the sorting of the grain-size distribution: the larger the standard deviation the weaker the sorting. Thus, the summer samples were characterized by a weaker sorting than the winter samples.

The grain size for which the grain-size distribution shows the highest frequency is called the modal grain size (Basu and DasGupta, 1997). The three year grain-size time-series mainly exhibits unimodal grain-size distributions (Fig. 3) which are a typical feature of aeolian sediments (Pye, 1987). Bimodal grain-size distributions are evident for ~7% of the samples and were only observed for sediment-trap samples with a relatively long sampling interval of 21 or 23 days (not shown). The modal grain sizes ranged from ~10 to ~55  $\mu\text{m}$  in the entire material analyzed for this study (Table 1). In a seasonal plot of modal grain sizes of the upper trap samples (Fig. 4a), the summer samples exhibited generally coarser modal grain sizes than the winter samples. The modal grain sizes peaked during summer with a maximum of 55  $\mu\text{m}$ . Furthermore, a larger spread in the modal grain sizes for the summer and spring samples was evident. The seasonal cycle was underlain by 'background dust' having modal grain sizes of 10–25  $\mu\text{m}$ . Larger modal grain sizes of >25  $\mu\text{m}$  can be found throughout the year. However, they are more abundant during spring and summer. Similar to the upper trap series the modal grain sizes of the lower trap series vary seasonally. However, peak modal grain sizes were shifted to late summer and early fall (not shown).

The online daily database of quasi-true color satellite images was checked for dust storm events by investigating each day of the sampling intervals of the upper trap CBi (Table 1). For 14 samples from site CBi with coarse modal grain sizes (>25  $\mu\text{m}$ ), deposition occurred during time intervals including a dust storm event, as illustrated by the satellite images. The modal grain sizes of these 14 samples deposited during dust storm events are displayed in blue color in Fig. 4a together with satellite images illustrating the dust storm events (Fig. 4c–f).

#### 4.1.2. Spatial variability

We compared modal grain sizes from the two trap sites in order to analyze possible changes in grain-size distributions with increasing distance from the dust sources. A clear spatial trend could be observed when comparing the mean modal grain size of the two sediment trap mooring sites (Fig. 5). A mean modal grain size of 24  $\mu\text{m}$  was calculated using the modal grain size values from three years of the upper trap series CBi 1–3. In contrast, the average modal grain size from two years of the lower trap series CB 15–16 was finer with 19  $\mu\text{m}$ . This difference is even larger when comparing the synchronous samples from the two upper trap series of CB 14 and CBi 1: the time-series from the upper trap, CBi 1, showed a mean modal grain size which was coarser by 7  $\mu\text{m}$  than in the upper trap time series CB 14 (Fig. 5). A mean sorting of 3  $\mu\text{m}$  was calculated for three years of the upper trap series CBi 1–3. The lower trap series CB 15 and 16 featured a better mean sorting of 2.7  $\mu\text{m}$  for a time frame of two years. The mooring CBi was located closer to the source than CB. Hence, the mean modal grain size decreases and the sorting increases with increasing distance from the African continent.

The lower sediment trap series from CB 16 showed peaks in the modal grain size which were similar to those observed for the upper trap series CBi 3. However, there was a time delay of one sampling cup between the peaks observed in the upper and the lower traps (Fig. 5). Two modal grain-size peaks in the lower trap of CB 16 that could not be recognized in the upper trap CBi 3 exhibited a bimodal grain-size distribution. The grain sizes of the upper trap series CBi 2–3 and lower trap series CB 15–16 have been correlated respectively. The bimodal distributions in the time series of CB 16 were excluded from the correlation, and the grain sizes as well as the lithogenic fluxes of the lower trap series were shifted

by one sampling interval. A correlation above a coefficient of determination ( $R^2$ ) of 0.2 is considered significant at the 99% confidence level for two-tailed probabilities. A positive correlation significant at the 99% confidence level ( $R^2 = 0.3$ ) was found for the modal, median and mean grain sizes and the standard deviations of the grain-size distributions (not shown).

#### 4.1.3. Seasonal variability

The sorting and modal grain sizes of the samples differed not only depending on the distance to the source but also depending on the season during which the dust was transported and deposited. For inter-seasonal comparison, mean sortings and modal grain sizes for each season have been calculated for the samples of the upper trap series at CBi 1–3. The samples that are characterized by dust-storm events occurring during the sampling interval have been included in the calculation. An advantage of the upper traps for seasonal investigation was the shorter transport pathway of the particles in the water column compared to the lower traps. It has been suggested that particles off Cape Blanc sink with 5  $\text{m d}^{-1}$  (Nowald et al., 2006) to 732  $\text{m d}^{-1}$  (Ploug et al., 2008a). This indicates that the upper traps will most likely show signatures from a recent dust storm while the deep ocean traps could have sampled dust particles from anything between a few weeks ago until several months ago. This complicates the correlation of the particle signal of the lower traps to environmental factors for a certain time interval. Therefore, the lower traps are not considered in this section.

A tendency to broader and coarser grain-size distributions of the summer samples as opposed to the winter samples is visualized in Fig. 6a. The mean modal grain size was around 29  $\mu\text{m}$  for the summer months as opposed to the winter months, which were characterized by a smaller mean modal grain size of 22  $\mu\text{m}$ . Whereas summer samples were characterized by a weaker mean sorting of 3.1  $\mu\text{m}$ , the winter samples featured a mean sorting of 2.9  $\mu\text{m}$ . Both spring and fall featured intermediate mean modal grain sizes of 23  $\mu\text{m}$ . Moreover, spring and fall samples were characterized by an intermediate mean sorting of 3.0  $\mu\text{m}$  (not shown).

The sorting of a grain-size distribution can also be derived by dividing the mean by the modal grain size (Fig. 6b). Values <1 indicated that the grain-size distribution was asymmetric and skewed to the left. For coarse samples (modal grain size >25  $\mu\text{m}$ ), an average sorting of 0.5 was derived for summer and 0.7 for winter. When taking into account dust-storm events during sampling intervals, a tendency towards weaker sorting was found for the anomalously coarse summer samples that deposited during sampling intervals including dust-storm events. Therefore, summer samples with anomalously coarse modal grain sizes and dust-storm events during the sampling interval were characterized by more asymmetric and left-skewed grain-size distributions.

#### 4.1.4. Interannual variability

The modal grain-size time series in Fig. 5 illustrates the interannual variability over the time period of three years. For all sediment trap samples studied, the modal grain size was at its maximum in September 2005 with ~55  $\mu\text{m}$  and at its minimum in February to March 2005 with ~10  $\mu\text{m}$ .

In Table 2 seasonal and annual averages of modal grain sizes and sortings are given for the upper sediment trap series CBi 1–3. The grain-size data of the site CB was not used for interannual comparison, because the data was obtained from one upper trap series and two lower trap series which biases a comparison. The largest year-to-year variation in mean modal grain sizes was observed for the spring season and the smallest spread for the fall season. In contrast, the interannual variation in the mean sorting was largest for the fall season and smallest for the winter season.

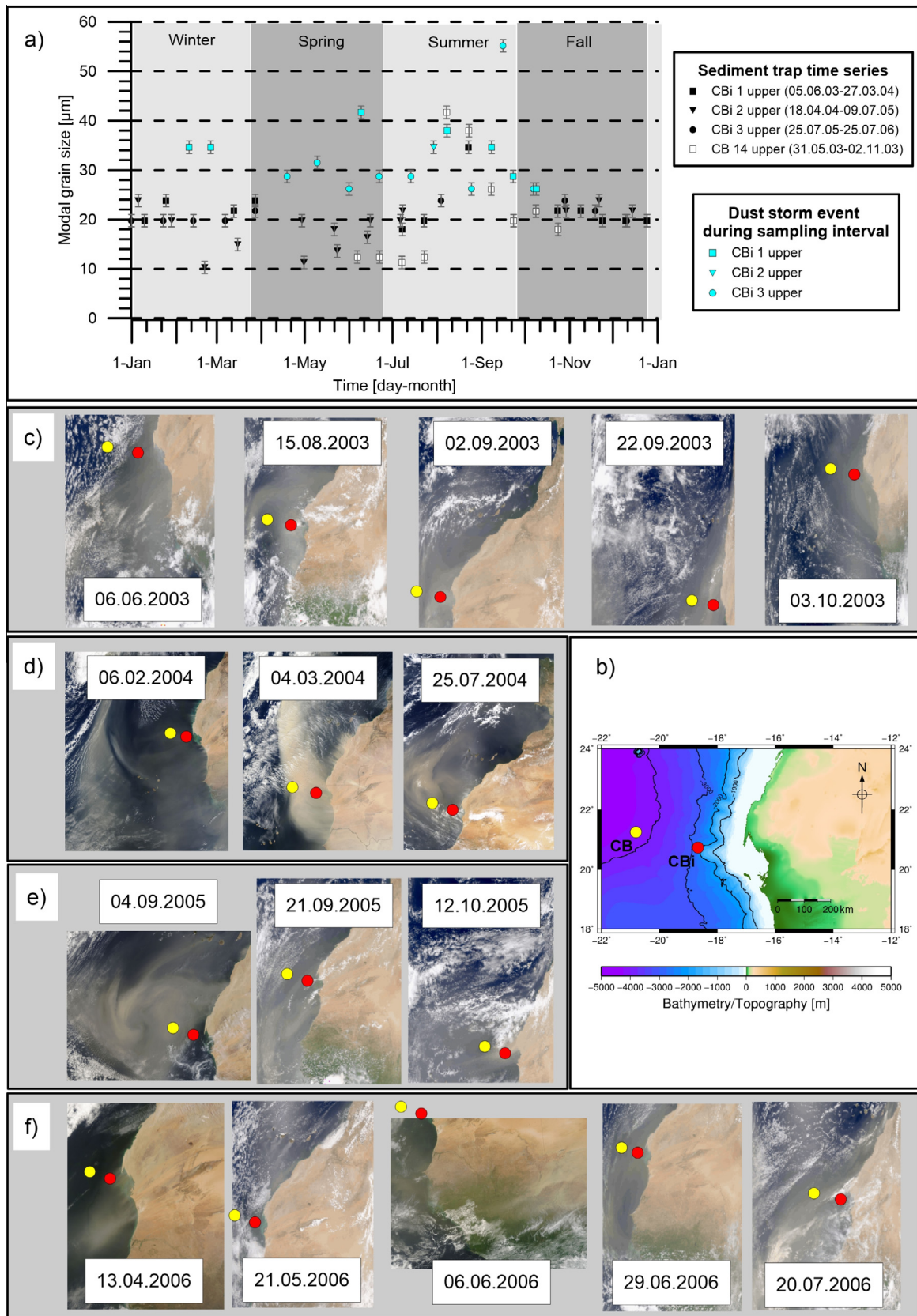


**Fig. 4.** (a) Results of grain-size analysis from the upper traps of sites CBi and CB. The modal grain sizes are plotted as a function of calendar day to investigate seasonality. Note that samples from different years are drawn within one figure. Coarse modal grain-size events ( $>25 \mu\text{m}$ ) of the CBi trap samples with dust storm events during the sampling interval are marked in blue. Symbols in the plot are drawn on the mid-point of the sampling interval. (b) Locations of the sediment trap moorings CB and CBi. (c–f) Quasi-true color satellite images of dust events occurring during sampling intervals with anomalously coarse dust ( $>25 \mu\text{m}$ ). (For interpretation of the references to color in this figure legend, the reader is referred to the web version of this article.)

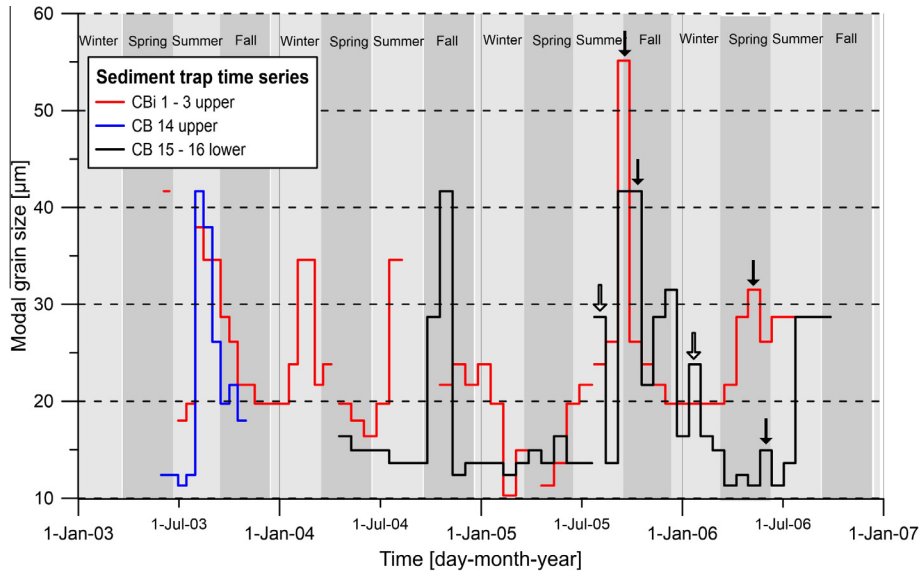


**Fig. 5.** Time series of modal grain size of the sites CB 14–16 and CBi 1–3. Black arrows indicate peaks in the modal grain size of the upper trap series CBi which can be observed in the lower trap series CB with a time delay. White arrows mark samples of the lower trap series CB which are characterized by a bimodal grain-size distribution.

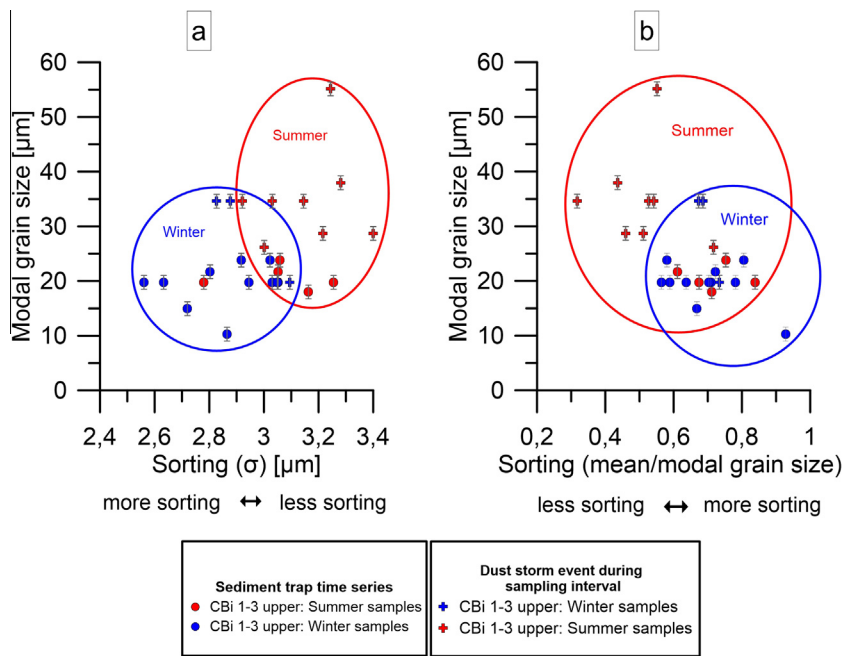


**Fig. 6.** Modal grain size versus sorting for the CBi 1–3 samples. Sorting can be given either by (a) the standard deviation of the distribution ( $\sigma$ ) or by (b) the mean divided by the modal grain size of the distribution. Dust storm events during the sampling interval are indicated by crosses.

A closer look at the modal grain sizes of the upper sediment trap series CBi 1–3 indicated that events with coarse modal grain sizes ( $>25 \mu\text{m}$ ) occurred not on an annual basis. In winter (February and March) 2004 two events were apparent but could not be found during the following two winter seasons. Coarse modal grain-size events during spring were evident for the years 2003 and 2006, however such events were absent for the years 2004 and 2005. In 2003 and 2005, coarse modal grain-size events were observed for the fall season as opposed to the year 2004 which lacked these coarse-mode events during fall (not shown).

#### 4.2. Wind-strength and precipitation

For comparison with concurrent atmospheric conditions (wind strength and precipitation) only the modal grain-size data of the

upper sediment trap series CBi 1–3 was used, because of the shorter time delay in the seasonal signal compared to the deeper traps. A time delay of two days was assumed for the particles to sink to the upper trap, from the ocean’s surface to 1300 m depth, since large zooplankton fecal pellets can sink with a speed of  $732 \pm 153 \text{ m d}^{-1}$  (Ploug et al., 2008b). Hence, a time shift of two days ahead in time was applied to the wind-strength and precipitation data to enable a comparison to the upper trap modal grain-size data for the respective sampling period.

In order to correlate the wind-strength data to the grain-size data, the mean zonal wind strength (for easterly directions only) at different atmospheric levels (1010–500 hPa,  $\sim 10$ –5500 m height) was calculated at the trap site for the respective sediment-trap sample time interval with a time shift of two days ahead in time. A correlation above a coefficient of determination



**Table 2**  
Annual mean and seasonal mean modal grain sizes and sorting ( $\sigma$ ) of the grain-size distributions from CBI 1–3 upper traps.

CBI trap series No.	Year	Winter	Spring	Summer	Fall	Annual mean (all samples)
<i>Mean modal grain size [<math>\mu\text{m}</math>]</i>						
CBI 1 upper	2003	–	42	29	23	–
CBI 1 + 2 upper	2004	26	19	27	22	24
CBI 2 + 3 upper	2005	17	15	31	23	22
CBI 3 upper	2006	20	27	29	–	–
<i>Mean sorting (<math>\sigma</math>) [<math>\mu\text{m}</math>]</i>						
CBI 1 upper	2003	–	2.9	3.2	2.7	–
CBI 1 + 2 upper	2004	2.8	2.9	2.9	2.9	2.9
CBI 2 + 3 upper	2005	2.9	2.9	3.1	3.4	3.1
CBI 3 upper	2006	3.1	3.3	3.3	–	–

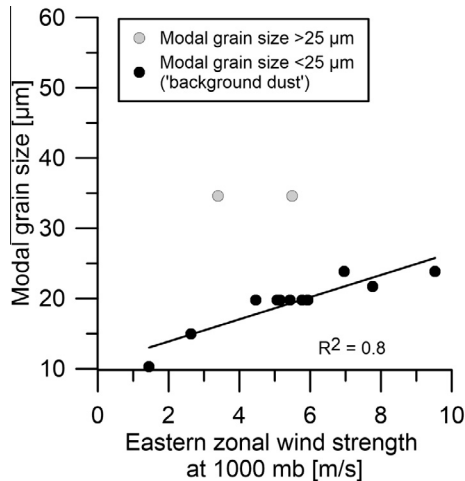


**Fig. 7.** Mean easterly zonal wind strength ( $22^{\circ}$  N,  $20^{\circ}$  W) for the respective sampling period (shifted two days ahead in time) at 1000 hPa vs. modal grain size for the winter samples of CBI 1–3. The modal grain size of the deposited aeolian sediments ('background dust') increased with increasing wind strength ( $R^2 = 0.8$ ).

( $R^2$ ) of 0.5 is considered significant at the 99% confidence level for two-tailed probabilities.

In Fig. 7 the modal grain sizes are plotted versus the corresponding mean easterly zonal wind speed at 1000 hPa (near-surface winds) for the winter season. A positive correlation was evident for the modal grain sizes of the background dust (10–25  $\mu\text{m}$ ) and five different low-level winds (wind strength at 1010 hPa, 1000 hPa, 950 hPa, 900 hPa and 850 hPa) with a coefficient of determination of  $R^2 = 0.8$  which is significant at the 99.9% confidence level. The two coarse modal grain size events ( $>25 \mu\text{m}$ ) during February and March 2004 were excluded from the regression since they are far off a linear relationship at any atmosphere level we checked. The linear regression line crosses the y-axis at  $y \approx 10 \mu\text{m}$ . The coefficient of determination decreases from  $R^2 = 0.8$  to  $R^2 = 0.5$  with increasing altitude in the atmosphere between the 850 hPa and 700 hPa levels. At the atmospheric levels 650 hPa and 500 hPa no significant correlation was observed at the 99% confidence level ( $R^2 < 0.5$ ). A significant positive correlation at the 99–99.9% confidence level ( $0.5 < R^2 < 0.8$ ) between the easterly zonal wind speed at 1000 hPa and the modal grain size (10–25  $\mu\text{m}$ ) was found when mean easterly wind strengths were calculated for the sampling period of the traps with time shift of 1 and 3–7 days ahead of the sampling time period. The best positive correlation was found when relating the modal grain size (10–25  $\mu\text{m}$ ) to the mean easterly wind speed at 1000 hPa during the sampling interval without a time shift of the wind speed data ( $R^2 = 0.9$ , significant at the 99.9% confidence level). During the other seasons no significant positive correlation between the modal grain sizes and the mean wind strength was observed ( $R^2 < 0.3$  which is below the 95% confidence level).

In order to study the influence of precipitation on the grain-size distribution of the deposited dust, the modal grain size of each sample was plotted versus the number of rain events (for precipitation  $>0.2 \text{ mm d}^{-1}$ ) around the CBI trap site during the respective sampling intervals, shifted two days ahead. Again, a correlation above a coefficient of determination ( $R^2$ ) of 0.5 is considered significant at the 99% confidence level for two-tailed probabilities. For the summer months a positive correlation ( $R^2 = 0.7$ ) was found to be significant at the 99.9% confidence level (Fig. 8a). In addition, the number of rain events were weighted against the sampling interval by dividing the respective number of rain events by the length of the respective sampling time interval. When weighting the number of rain events by the sampling interval of the traps the correlation was weaker but still evident ( $R^2 = 0.6$ ) at the 99% confidence level (Fig. 8b). A positive correlation significant at the 99% confidence level ( $R^2 > 0.5$ ) between the number of rain events above the mooring location and the modal grain size was also detected when no time shift was applied, and for time shifts of 1 or 3–7 days ahead in time of the meteorological data. No significant positive correlations with precipitation were detected for the other seasons at a confidence level of 99% ( $R^2 < 0.15$  which is below the 90% confidence level).

In general, dust deposited during dry summer intervals showed finer modal grain sizes than dust deposited during sampling intervals including rain events. Summer samples from wet sampling intervals are characterized by a larger number percentage of large grains around 30–100  $\mu\text{m}$  compared to summer dust deposited during dry intervals. In addition, the summer samples deposited during wet intervals are characterized by a larger number percentage of small grains around 0.4–0.7  $\mu\text{m}$ .

In Table 3 the meteorological data of the airport station at Nouadhibou, Mauritania, is provided of occasions when possible cold fronts moved towards the mooring locations. Cold fronts are characterized by a sudden increase in dew point temperature, surface pressure, wind speed and dust concentration and a decrease in temperature (Knippertz et al., 2007). The cold fronts identified based on these characteristics (Table 3) from the Nouadhibou airport station data occurred predominantly in the afternoon. Most importantly, the assumed cold fronts appeared during sampling time intervals with coarse modal grain sizes ( $>25 \mu\text{m}$ ) of the dust deposited offshore Cape Blanc. Please note that satellite quasi-true color images of dust storm events were available for the days 22.09.2003, 03.10.2003 and 12.10.2005 when cold fronts occurred (Fig. 4c and e).

## 5. Discussion

### 5.1. Grain-size distributions of proximal NW African dust

The predominantly unimodal grain-size distributions, typical for wind-blown sediments (e.g., Sarnthein et al., 1981) compare

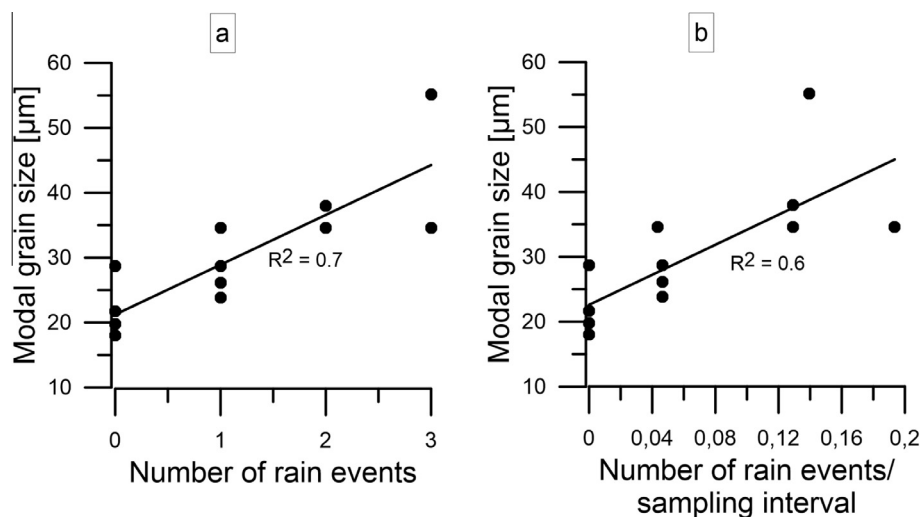


**Fig. 8.** Number of rain events ( $20^{\circ}33' - 20^{\circ}48' \text{ N}$ ,  $18^{\circ}36' - 18^{\circ}43' \text{ W}$ ) during the sampling time interval (shifted two days ahead in time) vs. modal grain size of the respective summer samples in Cbi 1–3: the modal grain size of the deposited aeolian sediments increases with increasing number of rain events without (a) and with (b) weighting by the sampling time interval.

**Table 3**  
Possible cold fronts identified using the hourly meteorological data from the airport station at Nouadhibou. Standard meteorological conditions (averages) during summer and fall are also given in the table.

Date [dd.mm.yyyy]	UTC Time [hh:mm]	Dew point [°C]	Temperature [°C]	Wind direction	Wind speed [m s <sup>-1</sup> ]	Pressure sealevel [mbar]	Visibility [km]	Comment
04.08.2003	15:00	19.9	24.5	360 (N)	9.8	1011.2	7	Dust or sand raised by wind
	16:00	23	24	360 (N)	11.8	1009.7	4	Dust or sand raised by wind
08.09.2003	12:00	17	32.2	20 (NNE)	5.1	1012.1	7	Dust or sand raised by wind
	13:00	22	31	140 (SE)	6.7	1012.5	7	Dust or sand raised by wind
22.09.2003	23:00	21	24	10 (NNE)	3.1	1013.5	11	
	00:00	23	27	130 (SE)	12.3	1016.5	4	Dust or sand raised by wind
03.10.2003	13:00	17	35	50 (NE)	3.6	1013.4	4	Dust or sand raised by wind
	14:00	20	30	330 (NNW)	7.2	1013.5	4	Dust or sand raised by wind
12.10.2003	00:00	18.2	23.8	20 (NNE)	9.8	1012.2	8	Dust or sand raised by wind
	01:00	21	24	20 (NNE)	10.3	1011.4	8	Dust or sand raised by wind
12.10.2005	20:00	19	31	40 (NE)	10.8	1012.6	2	Dust or sand raised by wind
	21:00	22.6	30.5	20 (NNE)	13.4	1014	10	Dust or sand raised by wind
<i>Standard meteorological conditions (averages)</i>								
Summer		20	24		7	1012.8	9	
Fall		16	23		6	1014.6	10	

well to other grain-size studies of mineral dust in the region (Holz et al., 2004; Koopmann, 1981; Mulitza et al., 2010; Ratmeyer et al., 1999a, 1999b; Skonieczny et al., 2013, 2011; Stuut et al., 2005; Tjallingii et al., 2008). Saharan dust sampled off western Africa on filters with a minimum temporal resolution of four hours, and dust sampled in dust collectors situated in Senegal with a minimum temporal resolution of seven days, also showed almost entirely unimodal grain-size distributions (Skonieczny et al., 2013, 2011; Stuut et al., 2005). Considering the lower temporal resolution (21–23 days) of time series CB 15–16 and Cbi 2–3, the collection of multiple dust outbreaks in one cup was likely and might explain the apparent existence of unusual bimodal grain-size distributions for these time-series. Bimodal grain-size distributions might be the result of the deposition of dust that has traveled short as well as long distances within the atmosphere or strongly varying wind speeds of the dust-transporting atmospheric layers during the sampling time interval.

The measured maximum particle sizes of Saharan dust (250 μm) (Fig. 3) deposited off Cape Blanc are in agreement with the recorded particle-size range of dust collected off the northwest African continent. Stuut et al. (2005) frequently observed particles with sizes up to 200 μm on dust filter samples collected along the western African coastline. Further, dust particles larger than 100 μm have

been recorded in sediment cores retrieved from the Cape Verde Terrace (Matthewson et al., 1995), off Morocco (McGregor et al., 2009) and off Cape Blanc (Filipsson et al., 2011) (Fig. 1). In addition, dust collected at an altitude of 170 m on air filters during an aircraft flight near Sal island revealed mica flakes with diameters up to 350 μm and quartz particles with diameters up to 90 μm (Glaccum and Prospero, 1980). Hence, the observed particle sizes of the dust deposited in the traps under investigation are within the typical size ranges of dust observed in the study area.

The grain-size distributions of this study showed a coarse shoulder between ~100 and 250 μm (Fig. 3). Stuut et al. (2005) also observed a coarse shoulder in the grain-size distributions for modern dust sampled offshore NW Africa. These authors argued that the coarse shoulder represented platy particles with large diameters such as micas. The Stokes terminal settling velocity is smaller for platy particles than for spherical particles of similar diameter (Santamarina and Cho, 2004). When taking into account the observed wind speeds of easterly direction in the study area, which are on average 5 m s<sup>-1</sup> and rarely exceeding 10 m s<sup>-1</sup>, it is unlikely that large spherical particles have been transported continuously to the sediment trap moorings. Therefore, the coarse shoulder in the grain-size distributions of the trapped dust has most likely been caused by large particles of the platy types.

The mean modal grain size of 19  $\mu\text{m}$  measured for the two years of the lower trap series CB 15–16 corresponded to the modal grain size of 19  $\mu\text{m}$  obtained for the surface sediments of sediment core GeoB 2912–2 (Ratmeyer et al., 1999b; Schulz et al., 1994). In addition, the mean modal grain size of 24  $\mu\text{m}$  obtained for the three years of the upper trap series CBI 1–3 is consistent with the value of 23  $\mu\text{m}$  found in surface sediments of sediment core GIK 12328–4 (Koopmann, 1981; Seibold, 1972). Further, a Q-mode analysis (Kipp, 1976) using the grain-size data of 84 surface sediments showed a maximum occurrence of a modal grain size of 24  $\mu\text{m}$  centred around 16–21°N and 20°E off NW-Africa (Sarnthein et al., 1981; Seibold, 1972), which is close to where the sediment trap mooring site CBI is positioned.

The modal grain size of the collected dust decreased from the proximal mooring site CBI to the more distal mooring site CB (Fig. 5). Tsoar and Pye (1987) showed that the distance ( $L$ ) traveled by a suspended particle obeying Stokes' Law is dependent on a transport component ( $Uz_\varepsilon$ ) as well as the gravitational settling speed of the particle ( $K^2D^4$ ). This dependency is expressed in the equation  $L = Uz_\varepsilon/K^2D^4$ , where  $U$  is the wind speed,  $\varepsilon$  is the coefficient of turbulent exchange,  $K = \rho_s g/18\mu$ , where  $\rho_s$  is the particle density,  $g$  is the acceleration due to gravity,  $\mu$  is the dynamic viscosity of air and  $D$  is the particle diameter (cm). Hence, the distance traveled by a particle decreases with decreasing wind speed and coefficient of turbulent exchange as well as increasing particle density and size. Assuming a comparable wind speed and coefficient of turbulent exchange between the two mooring sites, the distance a particle travels in the study area increases with decreasing size and density ( $L \sim 1/K^2D^4$ ). Thus, size-dependent gravitational settling was one major mechanism by which Saharan dust deposited at our sampling sites since the modal grain size decreased with increasing transport distance. The downward decrease in modal grain size of deposited Saharan dust offshore NW-Africa has been attributed to gravitational settling also previously (Darwin, 1846; Fütterer, 1980; Hellmann and Meinardus, 1901; Holz et al., 2004; Koopmann, 1981; Morales, 1986; Radczewski, 1939; Sarnthein et al., 1981; Semmelhack, 1934; Tsoar and Pye, 1987; Weltje and Prins, 2003) and is confirmed by our data. Hence, gravitational settling seems to be an overall mechanism by which the particles deposit in the eastern Atlantic (Prospero and Carlson, 1972).

## 5.2. Dust-storm events

The grain-size data of sediment trap mooring site CBI showed anomalously coarse modal grain-size events (>25  $\mu\text{m}$ ) simultaneously with dust storm events year-round (Fig. 4c–f). Spring was generally characterized by a high frequency of dust-storm events in large parts of Northern Africa as a consequence of the large temperature contrast between the cold mid- and high latitudes and quick heating of subtropical landmasses (Knippertz, 2014). As a result, energy for strong synoptic-scale disturbances is provided leading to cyclonic storms with sharp cold fronts (Knippertz, 2014; Rea, 1994; Schütz et al., 1981). Knippertz et al. (2007) described such a dust storm event from June 6th 2006 (see satellite image in Fig. 4f) and related it to density currents in the Atlas mountains with enhanced surface wind speeds. Intensified moist convection in mountainous regions and associated rainfall result in the evaporational cooling of hot and dry air masses below and consequent downhill acceleration of cold air which mobilizes dust along the fringes of the mountains (Knippertz et al., 2007). Thus, the development of density currents in the Atlas mountains might be a mechanism eventually leading to anomalously coarse dust deposits off Cape Blanc during spring.

The sediment trap samples collected during the summer season were characterized by frequent coarse grain-size events in combi-

nation with dust-storm events (Fig. 4c–f). In addition, cold fronts have been identified in Mauritania (Table 3) occurring during three sampling intervals with coarse modal grain-size events. The grain-size data of the upper trap time series CBI 1–3 further suggested that the modal grain size during summer was related to the frequency of rainfall events at the mooring location (Fig. 8a and b). A summer dust storm event occurring on July 17th 2006 during the sampling interval of an anomalously coarse dust sample has been described by Knippertz and Todd (2010). Satellite images showing dust storm events offshore NW Africa are available for July 19th (not shown), 20th (Fig. 4f), and 23rd (Fig. 2b) which might correspond to the documented event on July 17th 2006. The event on July 17th 2006 was characterized by a strong cyclonic vortex associated with an AEW that was situated over eastern Mali and traveled to western Mauritania the next day. As a result, easterly winds, to the northwest of the cyclonic center and convective cold pools, enabled the mobilization of dust which was subsequently transported offshore in the northeasterly flow (Knippertz and Todd, 2010). Moist convection is shown to be connected to the passage of AEW disturbances (Nicholson, 2009) and has been identified as a key mechanism for dust emission during the summer season (Knippertz et al., 2007; Knippertz and Todd, 2010; Svenningsson et al., 1997). The so called “haboobs” refer to large-scale dust-storm events which result from cold fronts caused by moist convection (Knippertz and Todd, 2012). At the leading edge of the cold front very sharp increases in wind speeds and particle concentrations typically occur (Knippertz, 2014). Field and laboratory wind tunnel experiments indicate that dust particles >20  $\mu\text{m}$  will be lifted up to 100 m in the atmosphere only with intense vertical air mixing (Pye, 1987). Hence, an increase in moist convection and surface wind speeds due to the passage of intensified AEW disturbances could have resulted in an enhanced entrainment of coarser particles into higher altitudes of the SAL. The rainfall events over the sediment trap sites (Fig. 8a and b) could be connected to these intensified AEW disturbances over the West African continent. During summer the dust front above the mooring locations can be observed to the east of a dense band of clouds which is in turn coupled to large-amplitude African disturbances (Carlson and Prospero, 1972) (Fig. 2b). Therefore, a possible enhanced entrainment of coarser particles into higher altitudes of the SAL as well as increased rainfall over the mooring sites could be both the result of intensified AEW disturbances traveling from the West African continent across the Atlantic Ocean.

Cold fronts were also identified for three anomalously coarse dust samples collected during fall 2003 and 2005 (Table 3). Hence, cold fronts could also be a mechanism resulting in the increased emission and transport of coarse particles offshore Cape Blanc during fall.

Two winter samples feature anomalously coarse modal grain sizes which were sampled during two prominent dust storm events occurring on February 3rd and March 4th 2004 (Fig. 4d). The observation of anomalously coarse winter samples has also been made by Charles Darwin on the H.M.S. Spey in 1838. He interpreted the dust to have been raised via a squall from the African coast (Darwin, 1846). The dust storm event during March 2004 (Fig. 4d) has been studied by Knippertz and Fink (2006). These authors explained that the dust storm event was caused by an intensification of a subtropical anticyclone over the Atlantic Ocean due to the penetration of cold air and strong winds into lower latitudes. The intensification of the anticyclone was accompanied by a cyclogenesis over the central northern Sahara, strong northerly winds over the northern Sahara and little rainfall. On March 3rd, near-surface winds were enhanced to 20  $\text{m s}^{-1}$  over the Sahara. It was a synoptic scale dust event considering that modeling results revealed dust sources ranging from Mauritania, Chad and Niger, Libya, Egypt and Sudan for the March 2004 dust event (Shao et al., 2010).

### 5.3. Dry versus wet deposition

We observed that dust deposited in summer during rain events shows a larger number percentage of submicron particles and a slightly larger number percentage of coarse particles (30–100  $\mu\text{m}$ ) compared to summer dust deposited in the absence of rain (not shown). In addition, the summer samples were generally characterized by a weaker sorting as opposed to the winter samples (Fig. 6a and b).

During summer, Saharan dust transport takes place within the SAL at altitudes of  $\sim 600$ – $5500$  m (Carlson and Prospero, 1972; Prospero and Carlson, 1970, 1972). At higher altitudes, submicron particles are more abundant since they have low settling velocities and can be more effectively transported to higher altitudes by turbulence as opposed to coarse particles (Tsoar and Pye, 1987). The settling of submicron particles from the atmosphere is controlled by Brownian diffusion and turbulent processes (Bergametti and Forêt, 2014). Brownian diffusion accounts for particles with diameters smaller than  $0.1$   $\mu\text{m}$  and can be neglected for the interpretation of our data since the detection minimum of the laser particle sizer is  $0.4$   $\mu\text{m}$ . The deposition velocity due to turbulent processes is at a minimum (Bergametti and Forêt, 2014). Consequently, the settling speeds of submicron particles might be too low in order to deposit from high altitudes by dry deposition. Therefore, wet deposition seems to be the general mechanism leading to elevated percentages of submicron particles in our summer dust samples. This is in accordance with the aircraft study of Carlson and Prospero (1972) suggesting that rainfall associated with the AEW disturbances leads to the wash-out of a dust fraction from the Saharan air entering the disturbance. The laser particle sizer records the diameter of a particle according to the axis which is oriented to the laser beam (Xu and Di Guida, 2003). Thus, the availability of platy particles results in the measurement of small and large diameters depending on which side of the particle has been oriented to the laser beam during particle size analysis (Xu and Di Guida, 2003). Consequently, a larger component of platy clay minerals in the summer samples may have led to generally broader particle-size distributions because both the short and the long axis of the clays were measured with the laser particle sizer.

We observed a weak positive relationship between the modal grain size and the lithogenic flux of the summer samples ( $R^2 = 0.4$ , not shown). Further, we observed a larger fraction of coarse particles in the summer samples deposited in time intervals including rain events (not shown). Hence, a larger fraction of coarse particles in the samples deposited in time intervals including rain events might be the result of a larger overall dust deposition during rain events. A few more particles  $>25$   $\mu\text{m}$  can result in a coarser modal grain-size value in the measured volume frequency distribution.

Two summer samples of the year 2003 showed larger modal grain sizes for the same time interval at site CB compared to site CBi (Fig. 5) which is counterintuitive when considering the general source-to-sink decrease in particle size due to gravitational particle settling. However, the sampling time intervals of these summer samples were characterized by rain events, which suggests that wet deposition can overprint the gravitational settling signal in the sediment trap samples.

### 5.4. Wind speed of the dust-transporting atmospheric layer

The data suggested a positive correlation between the lower atmosphere wind strength (1010–850 hPa) and the deposited grain sizes of the background dust (modal grain size  $<25$   $\mu\text{m}$ ) off Cape Blanc during the winter season (Fig. 7). The distance traveled by a suspended particle ( $L$ ) is given by the equation:  $L = U_{2e}/K^2 D^4$  (Tsoar and Pye, 1987). Assuming a constant transport distance,

the deposited particle size increases with increasing wind speed and coefficient of turbulent exchange and decreasing particle density ( $D^4 \sim U_{2e}/K^2$ ). Hence, presuming a constant source region, the transport of larger particles to the sediment-trap location was facilitated by increased wind strengths. Small particles can travel even further with increased wind velocities due to their small gravitational settling velocity. As a result, the modal grain size of the deposited dust was shifted towards larger sizes with increasing wind velocity (Fig. 7). During winter, dust is transported offshore Cape Blanc within the low-level trade winds with maximum velocities near the surface (Pye, 1987; Stuut et al., 2005) (Fig. 1). This is why the correlation between the modal grain size and the wind strength is best for lower atmospheric levels (1010–850 hPa). Dust mostly originates from Mauretania and the coastal areas of the western Sahara (Lange, 1982; Stuut et al., 2005). Hence, the transport distance is fairly constant during winter and the modal grain sizes of the deposited dust are solely determined by the trade wind pattern and strength.

The transport at higher altitudes during summer in the SAL may explain the low correlation between the modal grain sizes of the deposited Saharan dust and wind strength in the trade-wind layer during summer and fall. However, we suggest that moist convection in the source region could have triggered the entrainment of large particles to higher altitudes, and that wet deposition by rainfall was the principle factor controlling the particle-size distribution at our trap sites during summer.

### 5.5. Transport processes in the water column

The grain-size distributions and lithogenic fluxes of the upper traps CBi 2–3 were compared to the grain size distributions of the lower traps CB 15–16 (Fig. 5) to investigate vertical particle transport processes in the water column. This investigation is feasible because minimal horizontal particle advection occurs in the study area (Ratmeyer et al., 1999b; Stuut et al., 2005).

The modal and mean grain sizes and the standard deviations of the grain-size distributions correlated positively between the upper and the lower traps. A positive correlation is in accordance with the findings of Ratmeyer et al. (1999b) who investigated a one year synchronized grain-size time series of the upper and lower traps of the mooring site CB. They concluded that no significant particle alteration takes place during transport in the water column offshore Cape Blanc (Ratmeyer et al., 1999b). Possible scavenging and ocean currents did not alter the initial particle size distributions as observed in the upper traps significantly. This supports that dust particles are transported as aggregates and not as single particles in the deep ocean offshore Cape Blanc (Fischer and Karakas, 2009; Iversen et al., 2010; Ratmeyer et al., 1999b; Ternon et al., 2010).

The grain sizes of the upper trap also correlated positively to the lower traps when applying a time shift to the lower trap time series, which is necessary due to the large vertical distance between the traps. Correspondingly, the seasonal peak in the modal grain sizes of the lower trap series was shifted towards late summer to early fall. This indicated that the particle size signal was transferred with a time delay due to the transport of the particles in the water column. The peak in modal grain size (55  $\mu\text{m}$ ) in September 2005 of the upper trap series CBi 3 can be observed in the concurrent sample of the lower trap series CB 16 (42  $\mu\text{m}$ ), and with a time delay of one sampling interval in the next sample of the lower trap series CB 16 (42  $\mu\text{m}$ ) (Fig. 5). The two dust events occurring on 06 September 2005 (not shown) and 21 September 2005 (Fig. 4e) might be associated with the observed coarse modal grain-size peaks. Therefore, a time delay of 5 (min.) to 19 (max.) days can be derived for the particles of the first dust storm event to settle from the upper to the lower trap within the same sam-

pling interval and for the particles of the later dust storm event to settle into the next sampling interval of the lower trap at CB. As a result, the average vertical particle settling velocity was estimated to be from  $\sim 121$  to  $\sim 460$  m d<sup>-1</sup> between the upper and lower traps. The estimated particle sinking speeds were in the range of the sinking speeds determined by major flux correlations between the upper and lower traps at site CB which is 265 m d<sup>-1</sup> during summer (Fischer and Karakas, 2009).

The two bimodal grain-size distributions of the lower trap series CB 16 (Fig. 5) probably represent additional input of coarse particles since the coarse peak cannot be found in the upper trap series CBI 3. The additional input of coarse particles might be explained by downslope migration of heavy particles which has been modeled for the region offshore Cape Blanc (Karakas et al., 2006).

### 5.6. Implications for modeling and paleo-climatology

Measured data of dust emission for individual particle sizes are not available up to now (Shao, 2004). Further, model predictions of dust emission from different dust models are not consistent (Shao et al., 2011). The simplified dust emission scheme of Shao (2004) reflects that dust emission of a given particle size bin is proportional to the saltation mass transport and depends on the soil properties in the source regions. Our data suggest the emission and transport of a larger portion of large grains (>25  $\mu$ m), possibly due to increased atmospheric turbulence, vertical mixing of air, and surface wind speed in the source regions due to cyclonic storms, AEW disturbances, and cold fronts. Therefore, these processes should be represented in climate models, e.g. through sufficiently high resolution.

In addition to the dust emission schemes, there are still uncertainties with respect to the dust deposition parameters in dust models (Shao et al., 2011). Wet deposition is often estimated as a function of precipitation, scavenging and the airborne dust concentration. However, scavenging is dependent on parameters like the particle size or precipitation rates, and is therefore difficult to estimate. Our results showed that wet deposition of Saharan dust offshore Cape Blanc during the summer months is not only associated with increased deposition of submicron particles but also with increased percentages of large particles (>25  $\mu$ m). This should be taken into account in further developments of scavenging parameterizations.

The grain size of the terrigenous fraction of sediment core records has been used frequently as a measure of paleo-wind intensity (Parkin, 1974; Rea, 1994; Sarnthein et al., 1981). Further, the relative contributions of grain-size distribution end-members (Holz et al., 2007) as well as the median diameter (Matthewson et al., 1995) or coarse particle fluxes (Diester-Haass and Chamley, 1978) have been used as a proxy for wind intensity offshore NW Africa using sediment core samples. Our data confirm that the trade wind intensity can be related to modal grain sizes of the background dust (<25  $\mu$ m) deposited offshore NW Africa with a high coefficient of determination of  $R^2 = 0.8$  during the winter season. However, during the other seasons, dust mobilization and transport connected to convection on the continent, AEW and other synoptic-scale disturbances hinder the correlation between the trade winds and the background dust during these seasons. Sediment core records do not resolve seasonal variability and the sampling intervals rather represent time slices in the order of hundreds to thousands of years. As a result, the modal grain size of sediment core samples includes a signal of the mean winter trade-wind intensity, the intensity of moist convection on the continent during summer and fall as well as the intensity of dust storm events.

Year-round dust storm events as well as two or more rainfall events lead to a large-amplitude grain-size response. Thus, year-

round dust storm events and precipitation seem to be important environmental parameters with respect to the modal grain sizes of sediment core records.

The mean lithogenic flux of the anomalously coarse samples was calculated for each season. The results indicated that the mean lithogenic fluxes of the anomalously coarse samples were larger than the mean lithogenic flux of the background dust (not shown). Regarding the three years of the upper sediment trap series CBI under investigation coarse particles with a diameter larger than 25  $\mu$ m contributed to 35% of the total deposited lithogenic sediment (not shown). An interseasonal comparison revealed that summer was the season with the largest contribution of coarse particles to the total sediment with 12% and fall the season with the smallest contribution with 6% (not shown). Further, we observed a weak positive relationship between the modal grain size and the lithogenic flux of the summer samples (not shown). Consequently, summer is an important season with respect to the deposition of coarse particles. However, the other seasons play a significant role as well.

The mean and maximum of the lithogenic flux of the upper sediment trap series CBI 1–3 under investigation reached their peaks during spring (not shown). A pronounced seasonal variability in dust deposition fluxes with highest dust fluxes during winter/spring has been observed near the Senegalese margin (Skonieczny et al., 2013). A multidecadal particle flux record of the sediment trap mooring site CB located more offshore, however, indicates larger mean lithogenic flux during winter (Fischer et al., 2015). The anomaly of the winter lithogenic flux, however, is smaller than the observed interannual variability in the lithogenic fluxes (Fischer et al., 2015). Thus, winter and spring are important seasons with respect to the grain-size signal of sediment core records offshore northwestern Africa.

Consequently, the availability of dust-storm events during winter and spring may be the environmental factor that influences the variability in the grain-size distribution of sediment core records. However, coarse particle deposition during summer also plays an important role as reflected in the relatively large contribution of the lithogenic flux of coarse particles during summer to the total lithogenic flux. Therefore, the modal grain size of a sediment core sample offshore northwestern Africa should be mainly influenced by dust-storm events during winter/spring as well as dust-storm events and rainfall events during summer.

## 6. Conclusions

The grain-size distributions of the sediment trap mooring samples confirmed typical features of mineral dust blown offshore NW-Africa. Summer dust samples were characterized by generally coarser modal grain sizes and were less well-sorted. The grain-size distributions were influenced by various environmental factors depending on the season:

- Wind speed (winter): the NE trade-wind speed at the mooring location was positively correlated with the modal grain size of the deposited dust (for modal grain sizes <25  $\mu$ m).
- Precipitation (summer): increased particle fluxes due to wet deposition explain larger modal grain sizes of the samples. Cold fronts (haboobs) lead to the deposition of anomalously coarse dust samples (modal grain sizes >25  $\mu$ m).
- Episodic dust storm events (year-round): cyclonic dust storms and haboobs lead to the deposition of anomalously coarse dust (modal grain sizes >25  $\mu$ m).

The outcome of our study has implications for modellers and paleo-climatologists. The emission- and wet-deposition schemes

of dust models can benefit from the information that larger particles are emitted than usually accounted for by models and that summer rainfall leads to elevated percentages of submicron as well as large dust particles. Further, the modal grain size of sediment-core records obtained to reconstruct the climate history off NW-Africa is not only influenced by the paleo-trade-wind intensity, but also by the paleo-frequency of local precipitation and dust storm events, and by the paleo-intensity of moist convection in the source area.

## Acknowledgments

We thank the captains, crews and scientific teams of the research cruises with RV Meteor in 2003 (M58/2), RV Poseidon in 2004 (POS310), RV Meteor in 2005 (M65/2) and RV Poseidon in 2006 (POS344), during which the sediment traps were serviced. In addition, we thank Marco Klann for preparing and splitting the samples. JBS acknowledges funding from ERC Grant 311152 DUST-TRAFFIC. Funding is acknowledged from the German Science Foundation (DFG) through the DFG-Research Center/Cluster of Excellence “The Ocean in the Earth System”. For fruitful scientific discussions we further thank Prof. Dr. Dierk Hebbeln, Dr. Peter Knippertz and Dr. Gerlinde Jung.

## References

- Baker, E.T., Milburn, H.B., Tennant, D.A., 1988. Field assessment of sediment trap efficiency under varying flow conditions. *J. Mar. Res.* 46, 573–592.
- Basu, S., DasGupta, A., 1997. The mean, median, and mode of unimodal distributions: a characterization. *Theory of Probab. Appl.* 41, 210–223.
- Bergametti, G., Forêt, G., 2014. Dust deposition. In: Knippertz, P., Stuut, J.-B.W. (Eds.), *Mineral Dust*. Springer, Netherlands, pp. 179–200.
- Bleil, U., Schulz, H.D., Meinecke, G., Leitstelle, F., 2006. NW Africa: Cores, Traps, ROVs: Cruise No. 58: April 16–June 24, 2003, Dakar, Ponta Delgada. Leitstelle Meteor.
- Buesseler, K.O., Antia, A.N., Chen, M., Fowler, S.W., Gardner, W.D., Gustafsson, O., Harada, K., Michaels, A.F., van der Loeff, M.R., Sarin, M., Steinberg, D.K., Trull, T., 2007. An assessment of the use of sediment traps for estimating upper ocean particle fluxes. *J. Mar. Res.* 65, 345–416.
- Caquingon, S., Gaudichet, A., Gomes, L., Legrand, M., 2002. Mineralogy of Saharan dust transported over northwestern tropical Atlantic Ocean in relation to source regions. *J. Geophys. Res.* 107, 4251.
- Carlson, T.N., Prospero, J.M., 1972. The Large-scale movement of Saharan air outbreaks over the Northern equatorial Atlantic. *J. Appl. Meteorol.* 11, 283–297.
- Darwin, C., 1846. An account of the fine dust which often falls on Vessels in the Atlantic Ocean. *Quarterly J. Geol. Soc. London* 2, 26–30.
- Diaz, H.F., Carlson, T.N., Prospero, J.M., Office, E.R.L.W.M.P., 1976. A study of the structure and dynamics of the Saharan air layer over the northern equatorial Atlantic during BOMEX. Weather Modification Program Office, Environmental Research Laboratories.
- Diester-Haass, L., Chamley, H., 1978. Neogene paleoenvironment off NW Africa based on sediments from DSDP Leg 14. *J. Sediment. Res.* 48.
- Dobson, M., 1781. An account of the Harmattan, a singular African wind. *Philos. Trans. R. Soc. Lond.* 71, 46–57.
- Filipsson, H.L., Romero, O.E., Stuut, J.-B.W., Donner, B., 2011. Relationships between primary productivity and bottom-water oxygenation off northwest Africa during the last deglaciation. *J. Quat. Sci.* 26, 448–456.
- Fischer, G., Dormer, B., Ratmeyer, V., Davenport, R., Wefer, G., 1996. Distinct year-to-year particle flux variations off Cape Blanc during 1988–1991: relation to d18O-deduced sea-surface temperatures and trade winds. *J. Mar. Res.* 54, 73–98.
- Fischer, G., Karakas, G., 2009. Sinking rates and ballast composition of particles in the Atlantic Ocean: implications for the organic carbon fluxes to the deep ocean. *Biogeosciences* 6, 85–102.
- Fischer, G., Romero, O., Merkel, U., Donner, B., Iversen, M., Nowald, N., Ratmeyer, V., Ruhland, G., Klann, M., Wefer, G., 2015. Deep ocean mass fluxes in the coastal upwelling off Mauritania from 1988 to 2012: variability on seasonal to decadal timescales. *Biogeosciences Discussions* 12.
- Fischer, G., Ruhland, G., 2008. Report and preliminary results of Poseidon cruise 344 (POS344), Leg 1 & Leg 2, Las Palmas-Las Palmas, 20.10. 2006–02.11. 2006 & 04.11. 2006–13.11. 2006.
- Fischer, G., Wefer, G., 1991. Sampling, preparation and analysis of marine particulate matter. *Geoph. Monog. Ser.* 63, 391–397.
- Fütterer, D., 1980. Sedimentation am NW-afrikanischen Kontinentalrand: Quantitative Zusammensetzung und Verteilung der Siltfraktion in den Oberflächensedimenten. *Meteor-Forschungsergebnisse* C, 15–60.
- Glaccum, R.A., Prospero, J.M., 1980. Saharan aerosols over the tropical North Atlantic – mineralogy. *Mar. Geol.* 37, 295–321.
- Goudie, A.S., Middleton, N.J., 2001. Saharan dust storms: nature and consequences. *Earth Sci. Rev.* 56, 179–204.
- Hamilton, R.A., Archbold, J.W., 1945. Meteorology of Nigeria and adjacent territory. *Quarterly J. Geol. Soc. London* 71, 231–265.
- Hellmann, G., Meinardus, W., 1901. Der grosse Staubfall vom 9. bis 12. Maerz 1901 in Nordafrika, Sued-und Mitteleuropa, Behrend.
- Helmke, P., Romero, O., Fischer, G., 2005. Northwest African upwelling and its effect on offshore organic carbon export to the deep sea. *Global Biogeochem. Cycles* 19, 15.
- Holz, C., Stuut, J.-B.W., Henrich, R., 2004. Terrigenous sedimentation processes along the continental margin off NW-Africa: implications from grain-size analyses of surface sediments. *Sedimentology* 51, 1145–1154.
- Holz, C., Stuut, J.-B.W., Henrich, R., Meggers, H., 2007. Variability in terrigenous sedimentation processes off northwest Africa and its relation to climate changes: inferences from grain-size distributions of a Holocene marine sediment record. *Sed. Geol.* 202, 499–508.
- Huneus, N., Schulz, M., Balkanski, Y., Griesfeller, J., Prospero, J., Kinne, S., Bauer, S., Boucher, O., Chin, M., Dentener, F., Diehl, T., Easter, R., Fillmore, D., Ghan, S., Ginoux, P., Grini, A., Horowitz, L., Koch, D., Krol, M.C., Landing, W., Liu, X., Mahowald, N., Miller, R., Morcrette, J.J., Myhre, G., Penner, J., Perlwitz, J., Stier, P., Takemura, T., Zender, C.S., 2011. Global dust model intercomparison in AeroCom phase I. *Atmos. Chem. Phys.* 11, 7781–7816.
- IPCC, 2007. *Climate change 2007: the physical science basis*. Cambridge University Press.
- Iversen, M.H., Nowald, N., Ploug, H., Jackson, G.A., Fischer, G., 2010. High resolution profiles of vertical particulate organic matter export off Cape Blanc, Mauritania: degradation processes and ballasting effects. *Deep Sea Res. Part I* 57, 771–784.
- Iversen, M.H., Ploug, H., 2010. Ballast minerals and the sinking carbon flux in the ocean: carbon-specific respiration rates and sinking velocities of macroscopic organic aggregates (marine snow). *Biogeosci. Discussion* 7, 3335–3364.
- Iversen, M.H., Robert, M.L., 2015. Ballasting effects of smectite on aggregate formation and export from a natural plankton community. *Mar. Chem.* 175, 18–27.
- Jickells, T.D., An, Z.S., Andersen, K.K., Baker, A.R., Bergametti, G., Brooks, N., Cao, J.J., Boyd, P.W., Duce, R.A., Hunter, K.A., Kawahata, H., Kubilay, N., laRoche, J., Liss, P.S., Mahowald, N., Prospero, J.M., Ridgwell, A.J., Tegen, I., Torres, R., 2005. Global iron connections between desert dust, ocean biogeochemistry, and climate. *Science* 308, 67–71.
- Jones, C., Mahowald, N., Luo, C., 2003. The role of easterly waves on African desert dust transport. *J. Clim.* 16, 3617–3628.
- Jung, E., Shao, Y., 2006. An intercomparison of four wet deposition schemes used in dust transport modeling. *Global Planet. Change* 52, 248–260.
- Karakas, G., Nowald, N., Blaas, M., Marchesiello, P., Frickenhaus, S., Schlitzer, R., 2006. High-resolution modeling of sediment erosion and particle transport across the northwest African shelf. *J. Geophys. Res. Oceans* 111.
- Kipp, N.G., 1976. New transfer function for estimating past sea-surface conditions from sea-bed distribution of planktonic foraminiferal assemblages in the North Atlantic. *Geol. Soc. Am. Mem.* 145, 3–41.
- Knippertz, P., 2014. Meteorological aspects of dust storms. In: Knippertz, P., Stuut, J.-B.W. (Eds.), *Mineral Dust*. Springer, Netherlands, pp. 121–147.
- Knippertz, P., Deutscher, C., Kandler, K., Müller, T., Schulz, O., Schütz, L., 2007. Dust mobilization due to density currents in the Atlas region: observations from the Saharan Mineral Dust Experiment 2006 field campaign. *J. Geophys. Res. Atmos.* 112.
- Knippertz, P., Fink, A.H., 2006. Synoptic and dynamic aspects of an extreme springtime Saharan dust outbreak. *Quarterly J. R. Meteorol. Soc.* 132, 1153–1177.
- Knippertz, P., Stuut, J.-B.W., 2014. *Mineral Dust a Key Player in the Earth System*. Springer, Dordrecht.
- Knippertz, P., Todd, M.C., 2010. The central west Saharan dust hot spot and its relation to African easterly waves and extratropical disturbances. *J. Geophys. Res. Atmos.* 115.
- Knippertz, P., Todd, M.C., 2012. Mineral dust aerosols over the Sahara: meteorological controls on emission and transport and implications for modeling. *Rev. Geophys.* 50.
- Koopmann, B., 1981. Sedimentation von Saharastaub im subtropischen Nordatlantik während der letzten 25.000 Jahre. *Meteor Forschungsergebnisse* C 35, 23–59.
- Krastel, S., 2006. Report and Preliminary Results of RV Meteor Cruise M65/2: Dakar-Las Palmas, 04.07.–26.07.2005. Forschungszentrum Ozeanränder, RCOM, Univ. Lange, H., 1982. Distribution of chlorite and kaolinite in eastern Atlantic sediments off North-Africa. *Sedimentology* 29, 427–431.
- Luo, C., Mahowald, N.M., del Corral, J., 2003. Sensitivity study of meteorological parameters on mineral aerosol mobilization, transport, and distribution. *J. Geophys. Res.* 108, 4447.
- Maher, B.A., Prospero, J.M., Mackie, D., Gaiero, D., Hesse, P.P., Balkanski, Y., 2010. Global connections between aeolian dust, climate and ocean biogeochemistry at the present day and at the last glacial maximum. *Earth Sci. Rev.* 99, 61–97.
- Mahowald, N.M., Luo, C., del Corral, J., Zender, C.S., 2003. Interannual variability in atmospheric mineral aerosols from a 22-year model simulation and observational data. *J. Geophys. Res.* 108, 4352.
- Martin, J.H., 1990. Glacial-interglacial CO<sub>2</sub> change: the iron hypothesis. *Paleoceanography* 5, 1–13.
- Martin, J.H., Gordon, R.M., Fitzwater, S.E., 1991. The case for iron. *Limnol. Oceanogr.* 36, 1793–1802.
- Matthewson, A.P., Shimmield, G.B., Kroon, D., 1995. A 300 kyr high-resolution aridity record of the North-African continent. *Paleoceanography* 10, 677–692.

- McGregor, H.V., Dupont, L., Stuut, J.-B.W., Kuhlmann, H., 2009. Vegetation change, goats, and religion: a 2000-year history of land use in southern Morocco. *Quatern. Sci. Rev.* 28, 1434–1448.
- Meinecke, G., 2005. Report and preliminary results of Poseidon cruise 310 (POS310), Las Palmas (Spain)-Las Palmas (Spain) April 12th–April 26th, 2004.
- Meyer, I., Davies, G.R., Vogt, C., Kuhlmann, H., Stuut, J.-B.W., 2013. Changing rainfall patterns in NW Africa since the Younger Dryas. *Aeolian Res.* 10, 111–123.
- Middleton, N.J., Goudie, A.S., 2001. Saharan dust: sources and trajectories. *Trans. Inst. Br. Geogr.* 26, 165–181.
- Mittelstaedt, E., 1991. The ocean boundary along the northwest African coast: circulation and oceanographic properties at the sea surface. *Prog. Oceanogr.* 26, 307–355.
- Morales, C., 1986. The airborne transport of Saharan dust: a review. *Clim. Change* 9, 219–241.
- Mulitza, S., Heslop, D., Pittauerova, D., Fischer, H.W., Meyer, I., Stuut, J.-B., Zabel, M., Mollenhauer, G., Collins, J.A., Kuhnert, H., Schulz, M., 2010. Increase in African dust flux at the onset of commercial agriculture in the Sahel region. *Nature* 466, 226–228.
- Nicholson, S.E., 2009. A revised picture of the structure of the “monsoon” and land ITCZ over West Africa. *Clim. Dyn.* 32, 1155–1171.
- Nowald, N., Iversen, M.H., Fischer, G., Ratmeyer, V., Wefer, G., 2015. Time series of in-situ particle properties and sediment trap fluxes in the coastal upwelling filament off Cape Blanc, Mauritania. *Progr. Oceanogr.* A 137, 1–11.
- Nowald, N., Karakas, G., Ratmeyer, V., Fischer, G., Schlitzer, R., Davenport, R.A., Wefer, G., 2006. Distribution and transport processes of marine particulate matter off Cape Blanc (NW-Africa): results from vertical camera profiles. *Ocean Sci. Discuss.* 3, 903–938.
- Parkin, D.W., 1974. Trade-winds during the glacial cycles. *Proc. R. Soc. Lond. Ser. A* 337, 73–100.
- Ploug, H., Iversen, M.H., Fischer, G., 2008a. Ballast, sinking velocity, and apparent diffusivity within marine snow and zooplankton fecal pellets: implications for substrate turnover by attached bacteria. *Limnol. Oceanogr.* 53, 1878–1886.
- Ploug, H., Iversen, M.H., Koski, M., Buitenhuis, E.T., 2008b. Production, oxygen respiration rates, and sinking velocity of copepod fecal pellets: direct measurements of ballasting by opal and calcite. *Limnol. Oceanogr.* 53, 469–476.
- Prospero, J.M., Bonatti, E., Schubert, C., Carlson, T.N., 1970. Dust in the Caribbean atmosphere traced to an African dust storm. *Earth Planet. Sci. Lett.* 9, 287–293.
- Prospero, J.M., Carlson, T.N., 1970. Radon-222 in North Atlantic trade winds. Its relationship to dust transport from Africa. *Science* 167, 974.
- Prospero, J.M., Carlson, T.N., 1972. Vertical and areal distribution of Saharan dust over the western equatorial North Atlantic Ocean. *J. Geophys. Res.* 77, 5255–5265.
- Prospero, J.M., Lamb, P.J., 2003. African droughts and dust transport to the Caribbean: climate change implications. *Science* 302, 1024–1027.
- Prospero, J.M., Nees, R.T., 1977. Dust concentration in the atmosphere of the equatorial North Atlantic: possible relationship to Sahelian drought. *Science* 196, 1196–1198.
- Pye, K., 1987. *Aeolian dust and dust deposits*. Academic Press, London.
- Radczewski, O.E., 1939. *Eolian deposits in marine sediments*.
- Ratmeyer, V., Balzer, W., Bergametti, G., Chiapello, I., Fischer, G., Wyputta, U., 1999a. Seasonal impact of mineral dust on deep-ocean particle flux in the eastern subtropical Atlantic Ocean. *Mar. Geol.* 159, 241–252.
- Ratmeyer, V., Fischer, G., Wefer, G., 1999b. Lithogenic particle fluxes and grain size distributions in the deep ocean off northwest Africa: implications for seasonal changes of aeolian dust input and downward transport. *Deep Sea Res. Part I* 46, 1289–1337.
- Rea, D.K., 1994. The paleoclimatic record provided by eolian deposition in the deep sea: the geologic history of wind. *Rev. Geophys.* 32, 159–195.
- Santamarina, J., Cho, G., 2004. Soil Behaviour: The role of Particle Shape, *Advances in Geotechnical Engineering: The Skempton Conference*. Thomas Telford, pp. 604–617.
- Sarnthein, M., Tetzlaff, G., Koopmann, B., Wolter, K., Pflaumann, U., 1981. Glacial and interglacial wind regimes over the eastern subtropical Atlantic and North-West Africa. *Nature* 293, 193–196.
- Schepanski, K., Tegen, I., Laurent, B., Heinold, B., Macke, A., 2007. A new Saharan dust source activation frequency map derived from MSG-SEVIRI IR-channels. *Geophys. Res. Lett.* 34.
- Scheuven, D., Schütz, L., Kandler, K., Ebert, M., Weinbruch, S., 2013. Bulk composition of northern African dust and its source sediments — a compilation. *Earth Sci. Rev.* 116, 170–194.
- Schulz, H., Bleil, U., Henrich, R., Segl, M., 1994. *Geo Bremen South Atlantic 1994, Cruise No. 29, 17 June–5 September 1994 METEOR-Berichte* 95, 338.
- Schütz, L., Jaenicke, R., Pietrek, H., 1981. Saharan dust transport over the North Atlantic Ocean. *Geol. Soc. Am. Spec. Pap.* 186, 87–100.
- Seibold, E., 1972. Cruise 25/1971 of RV “Meteor”: Continental margin of West Africa. General report and preliminary results. “Meteor” *Forschungsergebnisse*, C 10, 17–38.
- Semmelhack, W., 1934. Die Staubfälle im nordwest-afrikanischen Gebiet des Atlantischen Ozeans. *Ann. Hydr.* 62, 273–277.
- Shao, Y., 2004. Simplification of a dust emission scheme and comparison with data. *J. Geophys. Res.* 109.
- Shao, Y., Fink, A.H., Klose, M., 2010. Numerical simulation of a continental-scale Saharan dust event. *J. Geophys. Res. Atmos.* 115, D13205.
- Shao, Y., Wyrwoll, K.-H., Chappell, A., Huang, J., Lin, Z., McTainsh, G.H., Mikami, M., Tanaka, T.Y., Wang, X., Yoon, S., 2011. Dust cycle: an emerging core theme in Earth system science. *Aeolian Res.* 2, 181–204.
- Siegel, D.A., Granata, T.C., Michaels, A.F., Dickey, T.D., 1990. Mesoscale eddy diffusion, particle sinking, and the interpretation of sediment trap data. *J. Geophys. Res. Oceans* 95, 5305–5311.
- Skonieczny, C., Bory, A., Bout-Roumazielles, V., Abouchami, W., Galer, S.J.G., Crosta, X., Diallo, A., Ndiaye, T., 2013. A three-year time series of mineral dust deposits on the West African margin: sedimentological and geochemical signatures and implications for interpretation of marine paleo-dust records. *Earth Planet. Sci. Lett.* 364, 145–156.
- Skonieczny, C., Bory, A., Bout-Roumazielles, V., Abouchami, W., Galer, S.J.G., Crosta, X., Stuut, J.B., Meyer, I., Chiapello, I., Podvin, T., Chatenet, B., Diallo, A., Ndiaye, T., 2011. The 7–13 March 2006 major Saharan outbreak: multiproxy characterization of mineral dust deposited on the West African margin. *J. Geophys. Res.* 116, D18210.
- Stuut, J.-B.W., 2001. Late Quaternary Southwestern African Terrestrial-climate Signals in the Marine Record of Walvis Ridge, SE Atlantic Ocean, Faculty of Earth Sciences, Utrecht University, Utrecht, p. 128.
- Stuut, J.-B.W., Mulitza, S., Prange, M., 2008. Challenges to understanding past and future climate in Africa. *EOS* 89, 196.
- Stuut, J.-B.W., Zabel, M., Ratmeyer, V., Helmke, P., Schefuß, E., Lavik, G., Schneider, R. R., 2005. Provenance of present-day eolian dust collected off NW Africa. *J. Geophys. Res.* 110.
- Svenningsson, B., Hansson, H.-C., Martinsson, B., Wiedensohler, A., Swietlicki, E., Cederfelt, S.-I., Wendisch, M., Bower, K.N., Choulaton, T.W., Colville, R.N., 1997. Cloud droplet nucleation scavenging in relation to the size and hygroscopic behaviour of aerosol particles. *Atmos. Environ.* 31, 2463–2475.
- Syvitski, J.P.M., 1991. *Principles, methods and application of particle size analysis*. Cambridge University Press, Cambridge.
- Ternon, E., Guieu, C., Loÿe-Pilot, M.D., Leblond, N., Bosc, E., Gasser, B., Miquel, J.C., Martín, J., 2010. The impact of Saharan dust on the particulate export in the water column of the North Western Mediterranean Sea. *Biogeosciences* 7, 809–826.
- Tjallingii, R., Claussen, M., Stuut, J.-B.W., Fohlmeister, J., Jahn, A., Bickert, T., Lamy, F., Rohl, U., 2008. Coherent high- and low-latitude control of the northwest African hydrological balance. *Nat. Geosci.* 1, 670–675.
- Tsoar, H., Pye, K., 1987. Dust transport and the question of desert loess formation. *Sedimentology* 34, 139–153.
- Weltje, G.J., Prins, M.A., 2003. Muddled or mixed? Inferring palaeoclimate from size distributions of deep-sea clastics. *Sed. Geol.* 162, 39–62.
- Xu, R., Di Guida, O.A., 2003. Comparison of sizing small particles using different technologies. *Powder Technol.* 132, 145–153.
- Yu, E.F., Francois, R., Bacon, M.P., Honjo, S., Fleer, A.P., Manganini, S.J., Rutgers van der Loeff, M.M., Ittekkot, V., 2001. Trapping efficiency of bottom-tethered sediment traps estimated from the intercepted fluxes of 230Th and 231Pa. *Deep Sea Res. Part I* 48, 865–889.
- Yu, H.B., Chin, M., Bian, H.S., Yuan, T.L., Prospero, J.M., Omar, A.H., Remer, L.A., Winker, D.M., Yang, Y.K., Zhang, Y., Zhang, Z.B., 2015. Quantification of trans-Atlantic dust transport from seven-year (2007–2013) record of CALIPSO lidar measurements. *Remote Sens. Environ.* 159, 232–249.